Atlantic Water influx in the Nordic Seas over the past 14.000 cal yr BP: Mg/Ca paleo temperature reconstructions

S. Aagaard-Sørensen[1*], K. Husum[1], M. Hald[1], T. Marchitto[2] and F. Godtliebsen[3]

[1] Department of Geology, University of Tromsø, 9037 Tromsø, Norway

[2] Department of Geological Sciences and Institute of Arctic and Alpine Research, University of Colorado, Campus Box 450, Boulder, Colorado 80309, USA

[3] Department of Mathematics and Statistics, University of Tromsø, 9037 Tromsø, Norway

[*]Author for correspondence: (e-mail: Steffen.Sorensen@uit.no)

Abstract

Mg/Ca-ratios have been used to reconstruct the temperature variations observed in the Atlantic Water carried towards the Arctic by the North Atlantic Current (NAC) and the West Spitsbergen Current (WSC). The investigated sediment cores are located in outer Andfjorden, Northern Norway (69°18´ N) and on the West Spitsbergen Slope, eastern Fram Strait (78˚54´ N). Both proxy records cover the past 14,000 cal yr B.P. The eastern Fram Strait Mg/Ca-ratios were measured on the planktic foraminiferal species *Neogloboquadrina pachyderma*. The Andfjorden Mg/Ca-ratios were measured on the benthic foraminiferal species *Melonis barleanus* and stable oxygen and carbon isotopes were measured on the benthic foraminifer *Cassidulina leavigata* in the Holocene part of the record. In the eastern Fram Strait little change in sea surface temperature ($SST_{Mg/Ca}$) is observed across the Late Glacial - Holocene boundary. Average temperatures were ca. 3.8°C. A temperature decline initiated in the early Holocene and culminated with lowest recorded averages of ca. 2.8°C at ca. 6,000 to 3,000 cal yr B.P. After 3,000 cal yr B.P. SSTs gradually increased reaching the highest recorded values averaging 5°C at ca. 1,100 cal yr B.P. to present. The $SST_{Mg/Ca}$ development correlates well with other Nordic Seas paleo records. The paleo records were governed by different forcing factors like fluctuations of insolation, North Atlantic Deep Water formation intensity, and poleward Atlantic Water advection due to changes of the atmospheric pressure systems. Furthermore, changes of the calcification season for *N. pachyderma* might have been a contributing factor to the observed signal. In Andfjorden bottom water temperatures ($BWT_{Mg/Ca}$) at ca. 500 meters water depth showed a strong influence from coastal waters

during the deglaciation. Relatively high $BWT_{Mg/Ca}$ of ca. 4.6°C was recorded during the Bølling/Allerød followed by a decline in the Younger Dryas showing average values around 3.3°C. $BWT_{Mg/Ca}$ increased markedly to ca. 7°C at 11,500 cal kyr B.P., when Atlantic Water started flowing into the Andfjorden. $BWT_{Mg/Ca}$ remained high and relatively stable with average values of ca. 11°C during the Holocene except for a small significant decrease observed from ca. 4,000 to 3,500 cal yr B.P. In general the Holocene $BWT_{Mg/Ca}$ development correlates with the decreasing insolation at 70°N.

1. Introduction.

In order to elucidate modern climate changes observed in Arctic and Subarctic environments, it is necessary to improve the knowledge regarding long term naturally occurring climate variations in the region (IPCC, 2007). The climate development in the Nordic Seas over the past 14.000 years have previously been studied in regard to numerous different proxies including distribution of diatoms (e.g. Koc et al., 1993), planktic foraminifera (e.g. Hald et al., 2007), benthic foraminifera (e.g. Ślubowska-Woldengen et al., 2008), ice rafted debris (IRD) (e.g. Bond et al., 1997), stable isotopes in planktic and benthic foraminifera (e.g. Bauch et al., 2001, Rasmussen, T. L. et al., 2007). All these studies and many more have elucidated that both the Late Glacial and the Holocene climate was variable. Many forcing factors and mechanisms are suggested to have governed the observed variability. These include orbital forcing resulting in changes in overall insolation forcing (Berger and Loutre, 1991), solar irradiance variability (Steinhilber et al., 2009), changes in atmospheric pressure systems giving rise to displacement of primary wind patterns (North Atlantic Oscillation index) (Hurrell, 1995), expansion and retraction of sea ice cover (Bond et al., 1997, 2001), North Atlantic Deep Water (NADW) formation variability (Oppo et al., 2003) and freshwater outburst from waning terrestrial ice sheets altering the thermohaline circulation (Teller et al., 2002; Alley and Ágústsdóttir 2005). An additional complication in the interpretation of paleoceanographic climate records is that surface and subsurface water masses respond differently to the intricate interactions of forcing mechanisms though the Holocene (e.g. Andersson et al., 2009).

In the north Atlantic and Nordic Seas observed variation in Atlantic Water inflow and composition during the Late Glacial and Holocene has been ascribed to and explained by various forcing factors and ecological parameters. These include atmospheric forcing (Risebrobakken et al., 2003; Giraudeau et al., 2004), ecology difference between zoo- and

phytoplankton (Jansen et al., 2008), orbitally driven seasonality changes (Hald et al., 2007; Jansen et al., 2008) and stratification due to surface water freshening (Giraudeau et al., 2004; Hald et al., 2007).

Studies have shown that Mg/Ca-ratios exponentially (or linearly) are positively correlated to water temperatures in both planktic (e.g. Elderfield and Ganssen, 2000; Kozdon et al., 2009) and benthic foraminifera (e.g. Lear et al., 2002; Kristjánsdóttir et al., 2007). The present study uses long time series of high resolution Mg/Ca-ratio measurements to calculate the temperature of the Atlantic Water transported toward the Arctic during the Late Glacial and Holocene. Similar long time series analyses of Mg/Ca-ratios have not previously been presented from Subarctic or Arctic environments. However, shorter time series utilizing the Mg/Ca method have been presented by Spielhagen et al. (2011) (eastern Fram Strait; *N. pachyderma*; 2,000 cal yr B.P. to present) and Rørvik et al. (submitted) (Malangen fjord, North Norway; *Cassidulina neoteretis*; 8,000 to 1,600 cal yr B.P.). SiZer analysis is used in the present study to identify significant changes taking place in the presented proxy records. Subsequent correlation to observed variations in North Atlantic and Nordic Sea paleo records is performed in order to elucidate on the forcing factors controlling the physical composition of the advected Atlantic Water. Mg/Ca-ratios have been measured at two strategic sites under the inflow of Atlantic Water via the North Atlantic Current (NAC) and West Spitsbergen Current (WSC). In Andfjorden, Northern Norway, Mg/Ca ratios measured on the benthic foraminifer *Melonis barleanus* were used to calculate bottom water temperatures ($BWT_{Mg/Ca}$). The bottom water conditions were further studied by analyzing stable isotopes in the benthic foraminifer *Cassidulina laevigata*. The combined $BWT_{Mg/Ca}$ and stable oxygen isotope ($\delta^{18}O$) values furthermore enable a tentative analysis of the relative bottom water salinity changes during the Holocene. In the eastern Fram Strait the Mg/Ca ratios measured on the planktic foraminifer *Neogloboquadrina pachyderma* formed basis for reconstructions of (sub) surface water temperatures ($SST_{Mg/Ca}$).

2. Oceanographic setting

The majority of the Atlantic Water is transported into the Nordic Seas over the Faeroe-Iceland Ridge at ~62°N (Hansen & Østerhus, 2000) (Fig 1). The Atlantic Water is advected northward in the North Atlantic Current (NAC; T>2°C, S>35) (Hopkins, 1991) adjacent to and below the Norwegian Coastal Current (NCC; T=3 to 13°C, S=30 to 34) (Aure and Strand, 2001) following the bathymetry along the Norwegian shelf (Fig 1). Presently the

Atlantic Water of the NAC has a thickness 500 to 600 m along the Norwegian continental shelf (Furevik et al., 2007). The NCC forms a westward thinning wedge over the Atlantic Water with a northward increasing depth varying between 50 to 150 m. The NCC is a mixture of Atlantic Water and fresh water originating from the Baltic Sea that is being continuously infused with run-off along the Norwegian coast (Aure and Strand, 2001). The shelf water enters into the Andfjorden (Fig 1) along the western slope and exits along the eastern slope (Nordby et al., 1999). At the studied core site the upper 125 m of the water column is influenced by the fresh NCC with salinities of ca. 33 and temperatures averaging 8°C (October 1999) (Fig 2). During summer the surface temperatures reach 12°C (Aure and Strand, 2001). The water masses from ca. 125 to 300 m water depth are a mixture of water from the NCC and Atlantic Water. Below 300 m water depth Atlantic Water dominates (T~7.8°C; S>35) (Fig 2).

The NCC continues northward and turns east into the SW Barents Sea alongside a branch of the NAC, the North Cape Current (Schauer et al., 2002). The other branch of the NAC continues further north along the west Barents Sea and Spitsbergen slopes where it is termed the West Spitsbergen Current (WSC) (Schauer et al., 2004) (Fig 1A & B). Atlantic Water (T: 3 to 7°C; S: 34.9 to 35.2) is carried by the WSC into the Arctic Ocean in the eastern part of the Fram Strait where it occupies the upper ~700 meters of the water column (Schauer et al., 2004; Walczowski et al., 2005) (Fig 1). In the Fram Strait the Atlantic Water submerges at ~78°N and is partly advected back south (Bourke et al. 1988) underneath the southward flowing East Greenland Current (Rudels et al. 2005) (Fig 1). The remaining Atlantic Water disperses into several sub currents in the Arctic Ocean (Manley, 1995). In the eastern Fram Strait modern temperatures in the melt water influenced surface layer (0 to 25 m) reach 8.2°C with a salinity at 34.95 (August 2006) (Fig 2). From 25 to 550 m Atlantic Water dominates (T~4°C; S=35 to 35.15). Below 550 m water depth Arctic Water is found (T= -1 to 1°C; S=34.9).

3. Material and methods

Sediment cores from Andfjorden, northern Norway and the West Spitsbergen slope were investigated (Fig 1, Table 1). The paleo record from Andfjorden is based on two sediment cores T79-51/2 and JM99-1200 (T79/JM99) previously studied by Hald and Hagen (1998) in addition to Ebbesen and Hald (2004). The lithology is described specifically by Vorren et al. (1983) and Plassen and Vorren (2002). The lithology of core MSM05/5-712-2 was described

onboard the R/V "MERIAN S. Merian" after coring. CTD profiles from both core site areas are shown in figure 2.

3.1. Age models

Age models have been constructed on the basis of ^{14}C AMS dates using linear interpolation between dated levels (Fig 3 & Table 2). The two cores from Andfjorden (T79-51/2 and JM99-1200) have been spliced together to form a single paleo record (Fig 3). The AMS dates from T79-51/2 and JM99-1200 were measured on various mollusc shells and fragments of shells (Table 2). Age models have previously been developed for these cores (Hald and Hagen, 1998; Ebbesen and Hald, 2004). In this study the radiocarbon dates were recalibrated with Calib version 6.0 (Reimer et al., 2005; Stuiver et al., 2005) using the marine calibration curve Marine09 (Hughen et al., 2004; Reimer et al., 2009). The standard reservoir correction of 400 years (R) was used in all calibrations. Furthermore the local reservoir age of 64±35 years (ΔR) was applied (Ebbesen and Hald, 2004) (Table 2) apart from during Younger Dryas (11 to 10 ^{14}C kyr) where a reservoir age of 200±50 years (ΔR) was applied (Bondevik et al., 1999, 2006) (Table 2). The two cores, T79-51/2 and JM99-1200, were spliced together at ca. 10.6 ^{14}C kyr where ^{14}C measurements almost overlap (Table 2). An age model was developed with linear interpolation between calibrated ages and the lowest date in T79-51/2 (at 318 cm) and the Vedde Ash layer in JM99-1200 (at 436.5 cm) (Grönvold et al., 1995). The sediment accumulation rate shows high and variable values on the late Glacial/Holocene transition (~35 to 424 cm/kyr) with low and stable values (<16 cm/kyr) after ~9.5 kyr (Fig 3). The age model of MSM05/5-712-2 was constructed on the basis of 10 AMS ^{14}C dates (Table 2). The AMS ^{14}C dates were carried out on planktic foraminiferal tests (*N. pachyderma*) from the upper 441cm of the sediment core (Aagaard et al. (in prep); Werner and Spielhagen (in prep); Giraudeau (in prep)). The AMS ^{14}C dates were calibrated using the latest calibration program and marine calibration curve (See above for details). The local reservoir age (ΔR=151±51) from Magdalenafjorden, Svalbard was used in the calibration (Mangerud and Gulliksen, 1975; Mangerud et al., 2006) (Table 2). The sediment accumulation rate is highest during Early Holocene and lowest in the early and late part of the studied time interval (Fig 3). All calibrated ages are an expression of years before present (1950). Late Glacial and Holocene chronostratigraphical zones used on figures and mentioned in the text follow Mangerud et al. (1974), Rasmussen, S. O. et al. (2007), Steffensen et al. (2008) and Walker et al. (2009).

3.2. Element analysis and contaminants

The sediment cores were sub sampled in 1 cm (MSM05/5-712-2) and 2 cm (T79-51/2 and JM99-1200) slices. The sediment was wet sieved at 63µm, 100µm and 1mm mesh sizes. For trace metal analysis of the Andfjorden record T79/JM99 (Fig 4) specimens were picked from the >100µm size fraction ensuring that specimens were of similar size. In T79/JM99 15 to 50 infaunal benthic foraminifera (*Melonis barleanus*) were picked per sample. Samples were picked at 4 cm resolution in T79-51/2 and at 5 to 10 cm resolution in JM99-1200 yielding a temporal resolution of ca. 8 to 300 yr/sample in the combined record. Two different phenotypes of *M. barleanus* were observed in the samples; a small "Slim" phenotype and medium sized "Transitional" phenotype following Quillmann & Jennings (in prep). Prior to 11,600 cal yr B.P. only the "Slim" phenotype was observed. This phenotype generally is small and most specimens were picked at the ca. 100 to 150µm size interval. During the Holocene the "Transitional" phenotype of *M. barleanus* was dominating and was picked at the >150µm size fraction.

In MSM05/5-712-2, West Svalbard Slope ca. 50 specimens per sample of the planktic foraminiferal species *N. pachyderma* were picked for trace metal analysis (Fig 5). Samples were picked at 2 cm and 3 cm resolution in the upper part (0 to 210cm) and lower part (210 to 441cm) of the sediment core, respectively, translating into a temporal resolution of ~36 to 120 yr/sample. In general only the most pristine specimens were selected during the picking procedure, i.e. very "dirty" specimens or specimens visibly influenced by dissolution were avoided. Furthermore specimens were picked within a relatively narrow size range (150 to 212µm) to reduce size dependant bias on the Mg/Ca measurements (Elderfield et al., 2002). After picking the foraminiferal tests were crushed and reductively (anhydrous hydrazine) and oxidatively (H_2O_2) cleaned (Boyle and Keigwin, 1985; Boyle and Rosenthal, 1996). Subsequently the samples were analyzed by magnetic-sector singlecollector ICP-MS, on a Thermo-Finnigan Element2 at the Litmann laboratory, University of Colorado operating with a long-term 1σ precisions of 0.54% for Mg/Ca measurements (Marchitto, 2006). Other trace element ratios simultaneously measured were: Mn/Ca, Fe/Ca and Al/Ca (Fig 4 & 5). After about 30 measured samples, a replicate analysis was carried out. The average reproducibility of sample splits was ±0.089 (T79-51/2 and JM99-1200) and ±0.039 mmol/mol (MSM5/5-712-2) in regards to Mg/Ca which on average is below <5% difference between duplicate measurements. Samples with <0.1 Ca recovery (<5µg $CaCO_3$) were rejected (Marchitto, 2006) (Fig 4 & 5). The Fe, Al and Mn (Fig 4 & 5) are tracers of contamination that might bias the Mg/Ca ratios (Barker et al., 2003). Fe and Al are tracers of detrital material

contamination (silicate minerals) and Mn is tracer of secondary diagenetic (Mn-rich carbonate coating (Boyle, 1983).

In regards to contamination the two present proxy records were treated differently. In the subarctic proxy record from Andfjorden (T79/JM99) the contamination thresholds for Fe, Al and Mn (>100µmol/mol) (Barker et al., 2003) are frequently transgressed (Fig 4). However, the Mg/Ca ratios are generally high in this record making the impact of contamination relatively smaller. Furthermore correlation between the Mg/Ca ratio and Fe/Ca, Al/Ca, Mn/Ca ratios is weak (Fig 6). Therefore only samples with low $CaCO_3$ recovery were omitted (Fig 4).

In the Arctic proxy record at west Spitsbergen slope (MSM05/5-712-2) all samples with >100 µmol/mol in regards to Fe, Al and Mn were omitted (Fig 5) because low Mg/Ca ratios are relatively more susceptible to contamination bias. Furthermore the weak but present correlation between Mg and Fe (R^2=0.25) and Mn (R^2=0.22) demand extra caution while Al show no significant correlation to Mg (R^2=0.01) (data not shown) (Fig 6).

3.3. Isotopic analysis

Stable isotope analysis was conducted at the (Leibniz Labor Kiel) using a Finnigan MAT 253 mass spectrometer with a reproducibility of ±0.04 for $\delta^{13}C$ and ±0.07 for $\delta^{18}O$. Results were calibrated to Pee Dee Belemnite (PDB) standard. The measurements were performed on average 34 specimens of the benthic foraminiferal species *Cassidulina laevigata* (n=161) (Fig 4). The specimens were picked at the >125µm size fraction at 2-cm intervals throughout core T79-51/2 (Andfjorden) covering most of the Holocene. The $\delta^{18}O$ values measured on *C. laevigata* (present study) and *C. reniforme* (Ebbesen and Hald, 2004) were corrected for a vital effect of 0.19‰ and 0.27‰ (Poole, 1994), respectively (Fig 4). The $\delta^{18}O$ values were corrected for ice volume effect where 0.11‰ change in $\delta^{18}O$ signal corresponds to a sea level change of 10 m (Fairbanks, 1989) (Fig 4).

3.4. Water temperature and relative salinity reconstruction

Sea water temperatures were calculated on Mg/Ca ratios measured in foraminiferal tests using species specific temperature equations (Fig 7). For *M. barleanus* an equation developed on the basis living specimens from shallow Iceland and Greenland shelves was used to calculate bottom water temperatures ($BTW_{Mg/Ca}$) (Fig 8) (Kristjánsdóttir et al., 2007): (Eq. 1) $Mg/Ca = 0.658 \pm 0.07 * \exp(0.137 \pm 0.020 * T)$. The equation is based on fauna living in

water temperatures of ~0 to 7°C which is equivalent or slightly below to the expected paleotemperatures.

The Mg/Ca ratios of *N. pachyderma* were calculated into sea surface temperatures ($SST_{Mg/Ca}$) using the linear equation of Kozdon et al. (2009): (Eq. 2) Mg/Ca (mmol mol^{-1}) = 0.13 (±0.037) * T + 0.35 (±0.17) (Fig 7). This equation is based on cross calibrated Mg/Ca and $\delta^{44/40}$ Ca proxy signals of *N. pachyderma* from Nordic Sea core top samples and covers a temperature range of ca. 3 to 6°C.

Tentative paleo bottom water temperatures based on isotopes ($BWT_{Isotope}$) were calculated using the equation of Shackleton (1974): (Eq. 3) $T=16.9 – 4 * (\delta^{18}O_c – \delta^{18}O_w)$, assuming constant $\delta^{18}O_w$ of 0.2 corresponding to a salinity of 34.5 in northern Norwegian fjords (Mikalsen et al., 2001) (Fig 7). Tentative relative changes in bottom water salinity were calculated using Eq.3. $\delta^{18}O_w$ (PDB) was estimated inserting the $BWT_{Mg/Ca}$ calculated on *M. barleanus* and $\delta^{18}O_c$ values of *C. laevigata* in Eq. 3. $\delta^{18}O_w$ (PDB) was subsequently converted to SMOW scale by adding 0.2‰. Translation of $\delta^{18}O_w$ (SMOW) to relative salinity change was done using the mixing line developed for Andfjorden by Austin and Salomonsen (in prep): (Eq. 4) $S = (14.88 + \delta^{18}O_{water, vs. V\text{-}SMOW}) / 0.43$. However, it must be noted that the Mg/Ca and $\delta^{18}O_c$ signals were measured on different species and therefore the bottom water salinity can only be translated into relative changes.

3.5. SiZer and spectral analysis

SiZer (Significance of Zero Crossings of the Derivative) analysis was conducted on separate and combined proxies from both records in order to elucidate and test statistical reliability of the major tends/developments in the records (Chaudhuri and Marron, 1999). The method was used to explore significant features in the proxy records. The method assumes that individual values are independent random variables. During the analysis a family plot is generated which is a smoothing of data at minimum to maximum resolution (Fig 8). By studying the wide range of resolutions (bandwidth, h), features in the curve can be identified at different levels of smoothing. Thereby the true underlying curves at particular levels of resolution are identified and insignificant natural variability is eliminated. The SiZer plot therefore gives a measure of the true variation observed in the proxy records. The SiZer map identifies patterns in the family plot by highlighting significant features (i.e. true decrease or increase in the curve) via a graphical display over age and scale (Fig 8). On proxies measured in Andfjorden the SiZer method was applied to the stable oxygen isotope ($\delta^{18}O$) record in T79-51/2 (Fig 8A) and to the $BWT_{Mg/Ca}$ record from combined cores T79-51/2 and JM99-1200 covering the

past 14 cal yr B.P. (Fig 8C). SiZer analysis was performed on the West Spitsbergen Slope $SST_{Mg/Ca}$ record measured using linear temperature equation (Fig 8D). The twoSiZer analysis was applied in order to test pairs of time series against each other at equal times on various timescales (Fig 8B: $\delta^{18}O$ - Mg/Ca ratios in core T79-51/2; Fig 8E: $BWT_{Mg/Ca}$, (Andfjorden) – $SST_{Mg/Ca}$ (West Spitsbergen slope). This approach enables direct comparison of relative rates and directions of change between individual proxy records.

Spectral analysis was conducted on various records in order to identify recurrent patterns. In the Andfjorden proxy records (T79-51/2 + JM99-1200) data were to scarce for analysis, while despite sufficient data points no significant periodicities were observed for the eastern Fram Strait record (MSM05/5-712-2) (data not shown).

4. Results

4.1. Subarctic record of benthic Mg/Ca ratios and stable isotopes (T79-51/2 and JM99-1200)

The trace metal analysis conducted at the benthic foraminifera *M. barleanus* is shown in Figure 4. The contamination with Mn, Fe and Al is quite extensive in T79-51/2 and JM99-1200 (Fig 4). However, no correlation between Mg/Ca and the contaminant indicators is found and the Mg/Ca values are thus assumed to be relatively unaltered by contamination (Fig 6). A few measurements prior to 11,700 cal kyr B.P. with low $CaCO_3$ recovery were omitted (Fig 4). From 14,000 to 11,600 all element analysis was conducted on *M. barleanus* (Slim) (Fig 4). The Mg/Ca values prior to ~12,800 cal yr B.P. average 1.26 mmol/mol and drop to 1.04 mmol/mol at ~12,800 to 11,600 cal yr B.P. After 11,600 cal kyr B.P and for the remainder of the record all analysis was conducted on *M. barleanus* (Transitional) (Fig 4). The two low values measured at 11,600 cal yr B.P. (~0.82 mmol/mol) are followed by a marked shift to high stable values, averaging 2.6 mmol/mol values at 11,400 to 10,000 cal yr B.P. (Fig 4). At ca. 10,000 cal yr B.P. the Mg/Ca values increase further to reach an average of 3.08 mmol/mol. At 10,000 to 400 cal yr B.P. the values show a slightly decreasing trend while some scatter between neighboring values is observed. Reconstructed $BWT_{Mg/Ca}$ shows low values before 12,800 cal yr B.P. (averaging 4.6°C) and a decline at 12,800 to 11,600 cal kyr B.P. (averaging 3.3°C) (Fig 7). The cold interval is followed by a large increase to ca. 10°C lasting from ca. 11,600 to 10,000 cal yr B.P. At 10,000 cal yr B.P. $BWT_{Mg/Ca}$ rise further to ca. 11.5°C and exhibit a slightly upward decreasing trend for the remainder of the record (Fig 7).

Stable isotopes measured on the benthic foraminiferal species *C. laevigata* in core T79-51/2 cover the time interval from 11,600 to 400 cal yr B.P (Fig 4). The $\delta^{18}O$ values are initially enriched with values averaging 3.6‰. A rapid transition is observed at 11,600 to 11,500 cal yr B.P. during which values decrease ca. 1.2‰. Subsequently an increase is observed with values fluctuating around 2.75‰ at 11,600 to 10,500 cal kyr B.P. At 10,500 cal yr B.P. values decrease further to ca. 2.5‰ followed by a steady increase to ca. 3‰ at the top of the record (Fig 4). The $BWT_{Isotope}$ estimated from the $\delta^{18}O$ signal (constant salinity) show a rapid increase from 1.5 to 8°C in 100 years (11,600 to 11,500 cal yr B.P.), before dropping ca. 2°C at 11,500 to 10,600 cal yr B.P. (Fig 7). At 10,600 cal yr B.P. values increase to ca. 7.5°C and subsequently decline steadily toward ca. 6°C (Fig 7). The $\delta^{13}C$ values initially fluctuate rapidly between -1.3 to -0.8‰ at 11,600 to 11,000 cal yr B.P. (Fig 4). After 11,000 cal yr B.P. the values gradually increase to average ca.
-0.3‰ at ca. 5,000 to 1,500 cal yr B.P. before a slight decrease is observed at the top 1000 years of the record (Fig 4). The relative salinity change shows an increase at 11,600 cal yr B.P. from -0.1‰ to averages of 1.2‰ corresponding to a ca. 3 unit salinity increase (Fig 7). Values decrease again to around 1‰ at 11,400 to 10,000 cal yr B.P. At 10,000 cal yr B.P. values increase ca. 0.5‰ (ca. 1.2 salinity units). The values average of ca. 1.5‰ for the rest of the record with the fluctuation amplitudes decreasing towards to top of the record (Fig 7).

4.2. Arctic record of planktic Mg/Ca ratios (MSM05/5-712-2)

The trace metal analysis conducted at the planktic foraminifera *N. pachyderma* is shown in Figure 5. Samples with low $CaCO_3$ recovery and/or high Mn, Fe and Al values (>100 µmol/mol) were omitted from further interpretation (Fig 5). At ca. 10,500 to 7,800 cal yr B.P. generally high Mn/Ca values are found (average ~80 µmol/mol). In this interval five samples exceeded the level of contamination and were omitted. During and in close temporal proximity to Younger Dryas Mn/Ca values are also intermittently elevated but only one sample exceeds the contamination threshold (Fig 5). Contamination level Fe/Ca values are found prior to ca. 10,300 cal yr B.P. at the top of the record (Fig 5). In total four samples were omitted due to Fe contamination. Al/Ca values are generally low (<50 µmol/mol) with only two samples at 7,900 and 200 cal yr B.P. omitted (Fig 5). The Mg/Ca values fluctuate between 0.6 to 1.1 mmol/mol with highest values prior to ca. 7,900 cal yr B.P. (average ~0.83 mmol/mol) and after ca. 2,500 cal yr B.P. (average ~0.89 mmol/mol) (Fig 5). Through the Late Glacial - Holocene transition Mg/Ca values fluctuate between 0.6 and 1.05 mmol/mol, but only little sustained change is registered. However, an early Holocene maximum could be

construed at ca. 10,500 to 7,900 cal yr B.P. with many high values above 0.95 mmol/mol and minimum values rarely below 0.75 mmol/mol. At 7,900 to 2,600 cal yr B.P. generally lower values are found (average ca. 0.75 mmol/mol) with especially low values with dampened variability found at ca. 5,200 to 2,600 cal yr B.P. (Fig 5). The $SST_{Mg/Ca}$ reconstruction (Fig 7) mirrors the Mg/Ca measurements (Fig 5) due to the linearity of the formula used (Kozdon et al., 2009). It must be cautioned that the equation of Kozdon et al. (2009) is based on samples that have not undergone the reductive cleaning step. The reductive cleaning lowers the Mg/Ca ratio by ca. 15% on average (Barker et al., 2003). However, despite the lowest $SST_{Mg/Ca}$ values (<2.5°C) trespassing of the lower sensitivity level of Eq. 2 the values can still be regarded as sound reflections of water temperatures as long as the cleaning procedures are kept in mind (Kozdon pers. com.). The sub $SST_{Mg/Ca}$ values fluctuate between 5.8 to 1.9°C (Fig 7). Highest values are found at ca. 10,500 to 7,900 cal yr B.P. (average 3.8°C) and after ca. 2,600 cal yr B.P. (average 4.1°C). Lowest sub $SST_{Mg/Ca}$ is recorded at 7,900 to 2,500 cal yr B.P. (average 3.1°C) (Fig 7).

4.3. SiZer analysis

The results of the SiZer analysis including family of smooths (h) are shown in figures 8A-E. The SiZer plot shows a map as a function of scale (y-axis: $\log_{10}(h)$) and location (x-axis: cal yr B.P.). The SiZer analysis yields an estimate of whether the curve at the specific point (x,h) has a derivative different from zero, i.e. if a true increase or decrease of the curve is observed. The SiZer analysis of the benthic $\delta^{18}O$ values from the Andfjorden record (T79-51/2) show a marked two step decrease at ca. 11,600 and 10,600 cal yr B.P. at multi decadal scale (Fig 8A). At ca. 9,000 cal yr B.P. an increase is observed which initially is seen in the multi centennial bandwidth and develops into a sustained increase at multi-millennial scale for the remainder of the record (Fig 8A). The twoSiZer plot is the result of subtracting the Mg/Ca record (reflecting temperature variations) from the $\delta^{18}O$ signal (reflecting temperature and salinity variations) (Fig 8B). The map shows that the $\delta^{18}O$ values decrease compared to Mg/Ca at ca. 11,500 to 7,000 cal yr B.P., with pronounced fast (multi centennial) relative change at ca. 10,700 and 10,000 cal yr B.P. After ca. 6,500 cal yr B.P. to the present the $\delta^{18}O$ values gradually increase relative to Mg/Ca (Fig 8B).

The SiZer analysis based on $BWT_{Mg/Ca}$ from the entire Andfjorden record (T79-51/2 and JM99-1200) shows a significant decrease within a century at ca. 12,800 cal yr B.P. (Fig 8C). At ca. 11,800, 11,000 and 10,000 cal yr B.P. marked centennial and bicentennial increases are observed and at ca. 4,000 to 3,000 cal yr B.P. a decrease is observed at millennial scale

bandwidth (Fig 8C). The SiZer analysis of the West Svalbard record of $SST_{Mg/Ca}$ shows a significant temperature decrease at ca. 10,000 to 6,000 cal yr B.P. and a rise after ca. 3,000 cal yr B.P. (Fig 8D). The twoSiZer plot compares the temperature development in Andfjorden ($BWT_{Mg/Ca}$) and at the West Spitsbergen Slope ($SST_{Mg/Ca}$) by subtracting the latter from the former (Fig 8E). At the beginning of the Holocene ca. 11,800 to 9,000 cal yr B.P. the $BWT_{Mg/Ca}$ in Andfjorden increase while the $SST_{Mg/Ca}$ on the west Spitsbergen slope remain stable. After ca. 3,500 cal yr B.P. the $BWT_{Mg/Ca}$ in Andfjorden is approximately constant while $SST_{Mg/Ca}$ at west Spitsbergen increases resulting in significant overall decreasing difference between the records (Fig 8E).

5. Discussion

The two Mg/Ca proxy records (Fig 4 & 5) and subsequent calculations into water temperatures (Fig 7) show very different patterns throughout the Late Glacial and the Holocene, despite that both are being derived from core sites under influence from Atlantic Water via the NAC and WSC (Fig 1). This difference is mainly that the Andfjorden and west Spitsbergen Slope records represent different depth intervals in the advected Atlantic Water, i.e. recording fluctuations of bottom water masses at 500 m and surface/subsurface water masses between 0 to 200 m water depth, respectively. The two core sites are also influenced by very different current systems. At the west Spitsbergen Slope the water column is influenced by Atlantic and Arctic Water masses while the Andfjorden is influenced by Atlantic Water and Coastal water masses (Fig 1). Furthermore the record from Andfjorden (60°N) is warmer compared to the record from the west Spitsbergen Slope (79°N) due to the heat loss to the atmosphere during the meridional advection of Atlantic Water (Fig 1). The difference between the records may also depict the increasing variability due to Arctic amplifications of the climatic signals towards the north (e.g. Hald et al., 2007). In Andfjorden the close proximity to land, glaciers and fresh water run-off during the deglaciation has significant impact on the studied bottom water environment. During the deglaciation the water depth in Andfjorden changed up to 30 m due to isostatic depression and eustatic sea level rise (Vorren and Moe, 1986; Fairbanks, 1989), while during most of the Holocene the water depth remained more or less constant. However, since the studied sediment cores were taken at ~500 m water depth the changing water depth is assumed to have been of minor importance in regards to $BWT_{Mg/Ca}$ and relative salinity change. The absolute $BWT_{Mg/Ca}$ values recorded during the Holocene in Andfjorden range between ca. 9 to 12.5°C (Fig 7).

Modern bottom water temperature was measured to 7.5°C in Andfjorden (October 1999) (Fig 2). Through the Holocene Atlantic Water inflow to the Nordic Seas at 62°N show stable temperatures of about 8°C at ca. 350 m water depth (Rasmussen and Thomsen, 2010) indicating that the absolute Holocene $BWT_{Mg/Ca}$ values calculated further north in Andfjorden are overestimated (Fig 7). However, preliminary parallel analysis of *M. barleanus* phenotypes from the Holocene part of the present record indicates that "Transitional" *M. barleanus* generate temperatures that are up to 3°C higher than "Slim" *M. barleanus* which suggests that the phenotypes are governed by different temperature equations (Quillmann & Jennings, unpublished data). Furthermore the "Transitional" specimens were relatively large (ca. 125-200 µm) compared to the "Slim" specimens (ca. 100-150 µm) which also may have played a significant role in the overall Mg/Ca ratios (e.g. Elderfield et al., 2002). The Andfjorden $BWT_{Mg/Ca}$ record is based on both "Slim" (ca. 14,000 to 12.800 cal yr B.P.) and "Transitional" (ca. 12,800 to 0,4 cal yr B.P) *M. barleanus*, hence the absolute values should be regarded with some caution (Fig 7).

In the eastern Fram Strait at the West Spitsbergen slope temperatures in the surface or near surface environment is recorded by *N. pachyderma*. This site was influenced by advected Atlantic Water and melt water from retreating glaciers (e.g. Elverhøi et al., 1995; Landvik et al., 1998; Birgel and Hass, 2004). The season and depth at which *N. pachyderma* calcifies is controlled by factors such as sea ice cover, proximity to sea ice margins and oceanic fronts, water mass distribution and food availability (Carstens et al., 1997; Volkmann, 2000). Furthermore recent investigations have shown that *N. pachyderma* during its life cycle migrates within the upper water column, reportedly being bound to a specific isopycnal layer (σ_t: 27.7 to 27.8) (Simstich et al., 2003; Kozdon et al., 2009). This means that *N. pachyderma* prefers gradually deeper habitats with increasing sea surface temperatures (Kozdon et al., 2009). Given the specific isopycnal layer disposition of *N. pachyderma*, the salinity of the water mass presumably also governs the depth habitat of *N. pachyderma*, i.e. decreasing salinities will, like increasing temperatures, make the species move to water masses with the preferred water density. Therefore the Mg/Ca ratios and subsequent sub $SST_{Mg/Ca}$ estimates cannot be regarded as originating from a specific depth but rather a varying depth interval generating a dampened temperature signal compared to the surface water mass temperature signal.

5.1. Evolution of $BWT_{Mg/Ca}$ in Andfjorden, northern Norway

The benthic foraminiferal record from Andfjorden is an expression of sea bed conditions at 500 m water depth. Andfjorden is influenced by the nearby Norwegian mainland and the interplay between inflowing Atlantic Water of the NAC and Norwegian Current Water (NCW) of the NCC (Fig 1). The $BWT_{Mg/Ca}$ from Andfjorden depicts a very prominent response to the final stages of the deglaciation (Fig 7). During Allerød at 14,000 to 12,800 cal yr B.P. temperatures were slightly elevated averaging 4.6°C (Fig 7). The increased inflow of Atlantic Water to the Nordic Sea during Bølling - Allerød (e.g. Koç et al., 1993) influenced the water masses in Andfjorden by increased mixing of Atlantic Water into NCC waters. The influence from Atlantic Water also resulted in elevated surface water temperatures and salinities allowing a subarctic planktic foraminiferal fauna to thrive in the surface water masses (Ebbesen and Hald, 2004).

At ca. 12,800 cal yr B.P. on the transition into Younger Dryas a significant $BWT_{Mg/Ca}$ decline of ca. 2°C is identified by the SiZer (Fig 8C). During Younger Dryas at 12,800 to 11,600 cal yr B.P. $BWT_{Mg/Ca}$ are low averaging ca. 3.3°C (Fig 7). The cold conditions indicate that Atlantic Water influenced the bottom water mass to a lesser extent probably due diminished meridional advection of Atlantic Water in the Nordic Seas (e.g. Koç et al., 1993). The low $BWT_{Mg/Ca}$ is supported by high stable oxygen isotope values measured on the Arctic benthic species *Cassidulina reniforme* (Fig 4) (Ebbesen and Hald, 2004). The generally cold conditions are also reflected by the planktic foraminiferal fauna that exhibits an almost complete dominance of the polar *N. pachyderma* in Andfjorden during this period (Ebbesen and Hald, 2004). The low $BWT_{Mg/Ca}$ during Younger Dryas was followed by a multi step warming. The first and largest step is marked by a significant $BWT_{Mg/Ca}$ increase of ca. 8°C (Fig 7) also identified by the SiZer at ca. 12,000 to 11,600 cal yr B.P. (Fig 8C). The warming is mirrored by a significant decrease in $\delta^{18}O$ values (from 3.5 to 2.7‰) (Fig 4) observed by the SiZer at ca. 11,600 cal yr B.P. (Fig 8A) which could indicate an increase in bottom water temperature and/or decrease in salinity. Rapid fluctuations between warm and cold periods at the end of Younger Dryas has been observed in both sea surface proxies and lake deposits in northern Norway (Ebbesen and Hald, 2004; Bakke et al., 2009). Similar "flickering" of the climate signal is not observed in the present $BWT_{Mg/Ca}$ record indicating that alternation between sea-ice cover and the influx of warm Atlantic Water did not influence the relatively more stable Atlantic Water inflow at 500 m water depth in Andfjorden. However, the calculated relative salinity clearly indicates a salinity increase at ca. 11,600 to 11,400 cal yr B.P. (Fig 7). This marked warming and relative salinity increase reflects the displacement of low temperature/low salinity NCW by warm and saline Atlantic Water from the NAC. A

similar large SST increase is recorded by the planktic faunal distribution change at ca. 11,600 to 11,000 cal yr B.P. (Hald et al., 2007).

The second significant $BWT_{Mg/Ca}$ increase identified by the SiZer at ca. 11,000 cal yr B.P. (Fig 8C) corresponds to a $BWT_{Mg/Ca}$ increase of ca. 1°C (Fig 7). The third significant $BWT_{Mg/Ca}$ increase of ca. 1.5°C (Fig 7) happened at ca. 10,000 cal yr B.P. (Fig 8C) and is predated by a significant $\delta^{18}O$ decrease at ca. 10,500 cal yr B.P. (Fig 8A) (from 2.7 to 2.5‰) (Fig 4). The elevated early Holocene $BWT_{Mg/Ca}$ combined with the increasing $\delta^{18}O$ values results in a marked relative salinity increased at ca. 10,000 cal yr B.P. which could indicate a general decrease in melt water runoff from the Norwegian mainland at this time (e.g. Eilertsen et al., 2005). The SiZer identifies a steadily increasing $\delta^{18}O$ after 9,500 cal yr B.P. and for the remainder of the record (Fig 8A) while $BWT_{Mg/Ca}$ after 10,000 cal yr B.P. remained relatively stable until a small but significant decrease occurred at ca. 4,000 to 3,500 cal yr B.P. (Fig 8C). The SST values inferred from planktic foraminifera show similar high but slightly increasing temperatures at 11,000 to 4,000 cal kyr B.P. (Hald et al., 2007). Contrary to the significant $BWT_{Mg/Ca}$ decrease at 4,000 cal kyr B.P. an increase of ca. 1°C is expressed by the planktic fauna (Hald et al., 2007). The stable carbon isotope ($\delta^{13}C$) measurements (*C. laevigata*) show an increasing trend during most of the Holocene and a slight decrease after 1,500 cal yr B.P. (Fig 4). This could indicate decreasing primary production in the water column and/or an increasingly improved ventilation state of the Atlantic Water mass. The former explanation is supported by the general decrease of the planktic foraminifera *Turborotalita quinqueloba* (Hald et al., 2007) which is a high productivity indicator species (Johannessen et al., 1994).

5.2. Evolution of sub $SST_{Mg/Ca}$ from the West Spitsbergen slope, eastern Fram Strait

The proxy record from the eastern Fram Strait is based on elemental ratios measured on the planktic foraminiferal species *N. pachyderma* expressing surface and/or surface near conditions the past 14,000 cal yr B.P. Across the Late Glacial/Holocene boundary at 14,000 to 10,000 cal yr B.P. some $SST_{Mg/Ca}$ scatter is observed (Fig 7), but no significant changes are identified by the SiZer analysis (Fig 8D). This apparent lack of a significant $SST_{Mg/Ca}$ changes could be ascribed to the capability of *N. pachyderma* to dwell at different depths depending on temperature and salinity (Kozdon et al., 2009) or a shift in seasonal production patterns (e.g. Farmer et al., 2008). The area was strongly influenced by sea-ice cover and ice berg transport prior to ca. 10,300 cal yr B.P. as observed by elevated IRD concentrations in the sediment and lowered foraminiferal fluxes (Aagaard-Sørensen et al., in prep).

Anomalously high Mg/Ca ratios have previously been identified in areas with sea ice cover (Nürnberg 1995; Meland et al., 2005) and could therefore be another possible explanation for the lack of any statistically significant temperature change across the boundary. Despite several proxies indicating change at ca. 10,300 cal yr B.P. in MSM05/5-721-2 (Aagaard-Sørensen et al., in prep) there seems to be only little or no change in the $SST_{Mg/Ca}$. The SiZer analysis confirms the lack of any significant changes taking place prior to ca. 10,000 cal yr B.P. but identifies a significant decline in $SST_{Mg/Ca}$ commencing at ca. 10,000 cal yr B.P. and ending at ca. 5,500 cal yr B.P. (Fig 8D). During the general temperature decline a rapid temperature drop of 0.5°C at ca. 7,700 cal yr B.P. (Fig 7 & 8D) and slightly elevated temperatures at 5,900 to 5,300 cal yr B.P. are the most pronounced features (Fig 7). $SST_{Mg/Ca}$ remain low and stable averaging 3°C at 5,300 to 3,200 cal yr B.P. with no significant changes observed in the SiZer (Fig 7 & 8D). This cold period is followed by a significant warming initiating at ca. 3,200 cal yr B.P. (Fig 8D). The warming is especially pronounced after 2,600 cal yr B.P. with only one short lived period at ca. 1,300 cal yr B.P. with temperatures <3°C (Fig 7). This late Holocene warming might be a depiction of generally elevated temperatures of the advected Atlantic Water mass or it could be linked to changes in foraminiferal calcification depth and/or season (e.g. Farmer et al., 2008; Kozdon et al., 2009).

5.3. Correlation to North Atlantic water masses and forcing factors

Temporal variation in the temperature, salinity and volume transport of Atlantic Water towards the Arctic Ocean can be observed by various proxies in different areas of the North Atlantic and the Nordic Seas. The variations are controlled by local, regional and global factors, which interplay to generate the observed signals.

In figure 7 the proxy records of the present study are compared to various forcing mechanisms. The North Atlantic Oscillation (NAO) winter index is defined by the atmospheric pressure difference between Iceland and the Azores. Positive index indicates larger difference resulting in stronger westerlies increasing wind driven Atlantic Water influx to the Nordic Seas yielding warm/wet conditions over NW Europe and vice versa (Negative NAO= less AW advection and cold/dry conditions) (Hurrell, 1995). The Holocene NAO index was deduced from glacier mass balances in maritime southern Norway (Nesje et al., 2001) (Fig 7E). Nine periods of increased ice rafting have been identified in the North Atlantic. Increased ice rafted debris (IRD) concentration denotes expansion of sea ice and increased ice berg transport in the North Atlantic (Bond et al., 1997) (Fig 7F). A close relationship between atmospheric ^{10}Be and sunspot frequency exists (Beer, 2001). High sun

spot frequency denotes high solar activity and increased solar irradiance. Measurements of ^{10}Be in ice core records have been used to estimate Holocene solar irradiation variability (Steinhilber et al., 2009) (Fig 7G). High δ^{13}C values measured on deep water benthic foraminifera in the northern North Atlantic (55°N, 15°W; water depth: 2,179 m) indicate periods of enhanced NADW formation, while low values indicate a slowing or shutdown of NADW formation (Oppo et al., 2003) (Fig 7H). Insolation is a measure of orbitally driven solar radiation energy received at various latitudes through time (Berger and Loutre, 1991) (Fig 7I).

5.3.1. Bottom water masses. Andfjorden.

Relatively high $BWT_{Mg/Ca}$ averaging 4.6°C is recorded during the Bølling - Allerød (14,000 to 12,800 cal yr B.P.) followed by a significantly colder Younger Dryas with temperatures averaging 3.3°C (12,800 to 11,600 cal kyr B.P.) in Andfjorden (Fig 7). During these periods the bottom water mass was probably strongly influenced by melt water runoff and ice berg release from the nearby Fennoscandian Ice Sheet. The relatively increased Bølling/Allerød $BWT_{Mg/Ca}$ correlates to enhanced inflow of Atlantic Water and opening of an ice free corridor along the coast of Norway (Koç et al., 1993; Klitgaard-Kristensen et al., 2001). The subsequent cooling during Younger Dryas correlates to the expansion of sea ice in the Nordic Seas (Koç et al., 1993). The Younger Dryas cooling generated a re-advance of the Fennoscandian Ice Sheet (Tromsø-Lyngen event) (Vorren and Plassen, 2002) and resulted in lowered overall primary productivity and a complete dominance of *N. pachyderma* in the surface water mass (Knies et al., 2003; Ebbesen and Hald, 2004). During early Younger Dryas a further 1°C $BWT_{Mg/Ca}$ decline is observed at 12,500 cal yr B.P. (Fig 7). This cooling correlates with the large sea ice expansion in the North Atlantic identified by Bond et al. (1997) (IRD event 9) (Fig 7F) and the high residual Δ^{14}C values (Reimer et al., 2005) indicating lowered oceanic ventilation and weakening of the Atlantic meriodional circulation system (Thornalley et al., 2010). The reduced Atlantic Water advection resulted in surface ocean cooling along the west coast of Norway and the Barents Sea shelf as inferred from radiolarian and foraminiferal fauna, diatom flora and elevated oxygen stable isotope values measured on planktic foraminifera (Koç Karpuz and Jansen, 1992; Hald and Aspeli, 1997; Dolven et al., 2002; Klitgaard-Kristensen et al., 2001; Birks and Koç, 2002; Risebrobakken et al., 2003; Sarnthein et al., 2003).

The proxy records south of Andfjorden depict a transition into warm Holocene oceanic conditions happening almost simultaneously with the significant $BWT_{Mg/Ca}$ (Fig 7B) and SST

increase in Andfjorden (Hald and Hagen, 1998; Ebbesen and Hald, 2007). This similarity indicates a link between varying Atlantic Water advection into the south-eastern Nordic Seas and the fluctuating temperatures observed in the Andfjorden proxy records on the Younger Dryas/Holocene transition. Furthermore the transition is almost concurrent (lacking ~200 years) with the $\delta^{18}O$ increase recorded in the NGRIP ice core (Rasmussen, S.O. et al., 2006) (Fig 7J). This implies that increased atmospheric temperatures, driven by the maximum summer insolation values (Berger and Loutre, 1991) (Fig 7I) and/or increased Atlantic Water advection into the North Atlantic influenced in the entire region. For the remaining part of the Holocene high and relatively stable $BWT_{Mg/Ca}$ (averaging ca. 11 °C) and SST inferred from planktic foraminiferal fauna is observed (Hagen, 1995; Hald et al., 2007) (Fig 7).
The bottom water stability is underscored by the tentative salinity estimate indicating relatively stable values after ca. 10,000 cal yr B.P. (Fig 7C). Despite its relative stability the $BWT_{Mg/Ca}$ shows a steady but minor decline throughout the Holocene correlating to the steady decline in summer insolation forcing (Berger and Loutre, 1991) (Fig 7I), while correlation to other forcing factors remains limited. A similar decline observed in the NGRIP ice core $\delta^{18}O$ signal confirms that the $BWT_{Mg/Ca}$ signal in Andfjorden draws its Holocene trend from a large scale orbitally driven north Atlantic atmospheric temperature development (Fig 7J). At ca. 4,000 cal yr B.P. a period of significant temperature decline is observed (Fig 7B & 8C) which correlates to the northern hemispheric Neoglacial cooling identified in numerous proxy records (e.g. Johnsen et al., 2001; Hald et al., 2007; Bakke et al., 2010). Elevated Holocene temperatures with low variability are also depicted by sub SST proxies along the Norwegian Shelf (Klitgaard-Kristensen et al., 2001; Dolven et al., 2002; Risebrobakken et al., 2003; Hald et al., 2007) showing the clear link between the poleward transport of Atlantic Water into the south eastern Nordic Sea and the water masses in Andfjorden. However, these records all depict slightly increasing or stable temperature during the Holocene implying influence on the sub surface temperatures from a range of factors that did not affect the $BWT_{Mg/Ca}$ in Andfjorden. These include seasonality of primary production/calcification (e.g. Volkmann, 2000; Farmer et al., 2008), changes in depth habitat (Simstich et al., 2003; Kozdon et al., 2009), influence of salinity and temperature on stratification (Hald et al., 2007) and/or varying influence from Arctic Water driven eastward by changing strength of the westerlies (Risebrobakken et al., 2003). Additionally the $BWT_{Mg/Ca}$ in Andfjorden during Holocene show almost no correlation to North Atlantic IRD events (Bond et al., 1997), changes in wind driven advection of Atlantic Water due to changing NAO (Hurrell, 1995; Nesje et al., 2001), solar irradiation (Steinhilber, et al., 2009)

or varying NADW production (Oppo et al., 2003) implying that temperature in the deep core (500 m) of the advected Atlantic Water was relatively unaffected by these forcing factors (Fig 7). The significant $BWT_{Mg/Ca}$ change found in Andfjorden at ca. 4,000 to 3,500 cal yr B.P. (Fig 8C) does, however, correlate with SST and BWT declines, inferred from foraminiferal fauna, observed in Atlantic Water advected through the Faroe-Shetland Channel at 62°N (Rasmussen and Thomsen, 2010).

5.3.2. Surface water masses. Eastern Fram Strait

Contrary to the Andfjorden $BWT_{Mg/Ca}$ record the eastern Fram Strait $SST_{Mg/Ca}$ record shows no significant response to the final stages of the deglaciation, but significant change during the Holocene (Fig 7 & 8). During Bølling/Allerød, Younger Dryas and well into the Holocene prior to ca. 10,500 cal yr B.P. *N. pachyderma* seems to have continuously recorded sub surface temperatures of a relatively warm inflowing Atlantic Water mass (Fig 4 & 7D). During the deglaciation, after ca. 15,000 cal yr B.P., a continuous subsurface influx of Atlantic Water to the Arctic Ocean has been described (Ślubowska-Woldengen et al., 2005; Rasmussen, T. L. et al., 2007). The Atlantic Water mass was situated below a melt water, sea ice and iceberg influenced surface water mass (Rasmussen, T. L. et al., 2007; Ebbesen et al., 2007; Aagaard-Sørensen et al., in prep). The presence of a fresh and cold surface layer may have facilitated a migration of *N. pachyderma* deeper into the warmer Atlantic Water and/or shift in the calcification season (e.g. Kozdon et al., 2009; Jonkers et al., 2010). The dominance of the fresh and cold surface layer diminished at ca. 10,500 cal yr B.P. where the Atlantic Water emerged at the surface and generated a marked SST increase along the West Spitsbergen slope as inferred from planktic foraminiferal fauna distributions (Sarnthein et al., 2003, Ebbesen et al., 2007; Aagaard-Sørensen et al., in prep). This marked SST increase along the West Spitsbergen slope is part of a south to north time-transgressive development in the Nordic Seas where the remnant cold water and sea ice pool gradually was displaced by Atlantic Water (Hald et al., 2007). However, the $SST_{Mg/Ca}$ recorded by *N. pachyderma* in the eastern Fram Strait remained relatively unaffected as the species kept recording approximately the same sub surface water mass conditions as before the Atlantic Water emerged at the surface.

A significant millennial to submillennial $SST_{Mg/Ca}$ decline commencing at ca. 10,000 cal yr B.P. and ending at ca. 5,500 cal yr B.P. is shown in figure 8E. This decline correlates with the decreasing summer insolation at 80°N during the period (Berger and Loutre, 1991) (Fig 7I). A wide spread early to middle Holocene cooling in the advected Atlantic Water has been

observed in various proxy records in the Nordic Sea including distribution patterns of diatoms (Koc et al., 1993; Birks and Koc, 2002) and benthic and planktic foraminifera (Hald and Aspeli, 1997; Hald et al., 2004; Knudsen et al., 2004; Ebbesen et al., 2007; Rasmussen, T. L. et al., 2007). The period at 7,700 to 6,000 cal yr B.P. exhibits some of the lowest recorded average sub $SST_{Mg/Ca}$ (3.1°C) during the Holocene matched only by even lower average sub $SST_{Mg/Ca}$ (2.9°C) at 5,200 to 2,700 cal yr B.P. (Fig 7D). Both these cold intervals correlate with marked periods of increased NADW formation (Oppo et al., 2003) (Fig 7H). Therefore it seems that during periods of stronger NADW production in the Nordic Sea the heat loss to the atmosphere was larger resulting in lower sub $SST_{Mg/Ca}$ values recorded in the part of the Atlantic Water advected further poleward in the Fram Strait. The cold period at 7,700 to 6,000 cal yr B.P. furthermore correlates to a period of low overall irradiance which could be a contributing factor to the $SST_{Mg/Ca}$ cooling (Steinhilber et al., 2009) (Fig 7). However, during the subsequent, even colder, period (5,200 to 2,700 cal yr B.P.) overall irradiation was high and rising and can therefore not contribute to explaining the stable low $SST_{Mg/Ca}$ values (Steinhilber et al., 2009) (Fig 7G). Instead the cold period at ca. 5,200 to 2,700 cal yr B.P. could be linked to weakened poleward Atlantic Water advection (Hurrell, 1995) as indicated by the frequently negative phase of the North Atlantic Oscillation (NAO) during the period (Nesje et al., 2001) (Fig 7E). In between the two relatively cold periods a minor warming at ca. 6,000 to 5,200 cal yr B.P. is observed in the present $SST_{Mg/Ca}$ (Fig 7D). An almost concurrent pattern of two cold periods bracketing a brief warmer period is also observed along the Barents Sea slope in SSTs inferred from planktic foraminiferal fauna distributions (Hald and Aspeli, 1997; Sarnhein et al., 2003). Furthermore Ebbesen et al. (2007) found Holocene minimum temperatures at ca. 8,000 to 3,000 cal yr B.P. with lowest values at 5,500 to 3,500 cal yr B.P. just south of the present core location (77°N) in the eastern Fram Strait. The similarity between the present and the above mentioned records indicate that areas under the axis of meridional Atlantic Water flux in the northeastern Nordic Seas were controlled by common forcing factors during the middle Holocene.

A significant warming in the WSC initiates at ca. 3,000 cal yr B.P. (Fig 8D). The warming is especially pronounced after 2,600 cal yr B.P. with only one short lived period at ca. 1,300 cal yr B.P. with temperatures <3°C (Fig 7D). This brief cooling coincides with the IRD event 1 (Fig 7F) (Bond et al., 1997). The warming trend is in contradiction to the low and declining insolation forcing at 80°N (Berger and Loutre, 1991) (Fig 7I). However, the period falls within a period of primarily positive NAO index values (like during the early Holocene) (Fig

7E) which could indicate stronger advection of Atlantic Water towards the North (Hurrell, 1995).

Furthermore the period at 2,600 to 1,400 cal yr B.P shows the strongest total solar irradiance during the Holocene, but the decline after 1,400 cal yr B.P to present (Steinhilber et al., 2009) does not correlate with the significantly increasing $SST_{Mg/Ca}$ (Fig 7) indicating that total solar irradiance probably was a subordinate driving mechanism. Reconstructed SSTs based on transfer functions from the eastern Fram Strait show a ca. 3°C increase at around 3,000 cal yr B.P. (Ebbensen et al., 2007). SST estimates deduced from zooplankton at ca. 67°N also show a late Holocene temperature increase commencing, however, at different times (Dolven et al., 2002; Risebrobakken et al., 2003). At this low latitude the proxy record based on radiolarians show increasing sub surface temperatures continue to the present (Dolven et al., 2002) while increases recorded by planktic foraminifera ended during the Little Ice Age (Risebrobakken et al., 2003). However, other proxy records indicate atmospheric and marine temperature stability or decline more in line with the low and declining insolation forcing (Berger and Loutre, 1991). These include the NGRIP ice core record (Vinther et al., 2006; Rasmussen, S. O. et al., 2006), SST estimates based diatom distributions the Nordic Seas (Koç Karpuz and Jansen, 1992; Koç et al., 1993; Andersen et al., 2004), summer temperatures based on pollen distribution in northern Scandinavia (Seppä et al., 2008), glacier advances in southern Norway (Nesje et al., 2001), BWT from north Iceland shelf derived from benthic Mg/Ca-ratios (Kristjánsdóttir et al., 2007), and indeed the present $BWT_{Mg/Ca}$ record from Andfjorden (Fig 7B & 8C).

The late Holocene warming possibly could be linked to the weaker seasonality of insolation (Berger and Loutre, 1991) (Fig 7I) narrowing the growing season for phytoplankton and foraminiferal calcification to late summer where the advected Atlantic Water was warmer. A shorter calcification season might also have been forced by increased and prolonged sea ice cover generating primary productivity blooms later in the season. Increased influence of sea ice in the eastern Fram Strait has been inferred from elevated IRD concentrations in the sediment recorded at the West Spitsbergen Slope after ca. 5,000 cal yr B.P. (Rasmussen, T. L. et al., 2007).

A striking feature observed in the present record is the larger variability of $SST_{Mg/Ca}$ from 2,500 cal yr B.P. to the present which probably also can be linked to more variable sea ice cover and/or to more variable Atlantic Water advection into the Nordic Seas as inferred from frequently fluctuating NAO index values (Nesje et al., 2001) (Fig 7E).

6. Conclusions

Mg/Ca element ratios were used to reconstruct bottom temperatures ($BWT_{Mg/Ca}$) and (sub) sea surface temperatures ($SST_{Mg/Ca}$) at two core sites under the influence of Atlantic Water in the Nordic Sea and the Fram Strait. The two proxy records investigated in the present study depict different temperature responses to known climatic periods through the Late Glacial and the Holocene.

The Andfjorden $BWT_{Mg/Ca}$ at ca. 500 m water depth measured on *M. barleanus* shows a pronounced response to the final stages of the glaciation due a close proximity to the waning Scandinavian Ice Sheet and strong influence from low salinity Norwegian Coastal waters. The Bølling/Allerød showed slightly elevated average temperatures (4.6°C) compared to the subsequent Younger Dryas period depicting lower average temperatures (3.3°C). At ca. 11,500 cal yr B.P. $BWT_{Mg/Ca}$ increased ca. 7°C as the seabed became flushed with Atlantic Water. The initial $BWT_{Mg/Ca}$ increase was followed by two minor increases at 11,000 (ca. 1°C) and 10,000 cal yr B.P (ca. 1.5°C). After the early Holocene $BWT_{Mg/Ca}$ increases the record remained relatively stable at around 11°C until ca. 3,500 cal yr B.P. where a small but significant decrease of ca. 0.5°C was recorded. The general stability of the Holocene bottom water composition was supported by oxygen isotope values measured on *C. laevigata*. The main forcing factor influencing the Holocene $BWT_{Mg/Ca}$ seems to be the overall decreasing insolation at 70°N.

The eastern Fram Strait sub $SST_{Mg/Ca}$ was measured on *N. pachyderma*. No significant sustained changes were observed in the $SST_{Mg/Ca}$, averaging ca. 3.8°C, during the Late Glacial and into the early Holocene possibly due to severe sea ice conditions in the area prior to ca. 10,300 cal yr B.P. A gradual decrease in $SST_{Mg/Ca}$ was observed at ca. 10,000 to 6,000 cal yr B.P. followed by sustained low temperatures averaging ca. 2.8°C recorded at ca. 5,500 to 3,000 cal yr B.P. The lowest recorded temperatures correlate to periods of stronger NADW production in the Nordic Sea. The late Holocene after ca. 3,000 cal yr B.P. depict a marked increase in $SST_{Mg/Ca}$, reaching an average of ca. 5°C the last 1000 year of the record. This significant late Holocene $SST_{Mg/Ca}$ increase possibly can be linked to stronger advection of Atlantic Water as indicated by positive NAO index values and/or a shift in calcification season for *N. pachyderma*.

Acknowledgements

This work has been carried out within the framework of the International Polar Year project "Arctic Natural Climate and Environmental Changes and Human Adaption: From Science to

Public Awareness" (SciencePub) funded by the Research Council of Norway and the Trainee School in Arctic Marine Geology & Geophysics, University of Tromsø and the Norwegian Science council. To these institutions we offer our sincere thanks. The core was collected onboard the R/V "MERIAN S. Merian" during the MSM05/5b expedition led by Dr. Gereon Budeus, Alfred Wegener Institute. Patrick Cappa assisted the laboratory work at INSTAAR, University of Colorado. Jan Petter Holm prepared the area map. R. Kozdon and T. L. Rasmussen contributed with constructive inputs to the manuscript. To these persons we offer our sincere thanks.

References

Aagaard-Sørensen, S., K. Husum, M. Hald, T. Marchitto, K. Werner, and R. Spielhagen (in prep), The Mg/Ca - temperature proxy applied in an Arctic paleoceanographic setting - a multiproxy study.

Alley, R. B. & A. M. Ágústsdóttir (2005) The 8k event: cause and consequences of a major Holocene abrupt climate change. *Quaternary Science Reviews,* 24**,** 1123-1149.

Andersson, C., F. S. R. Pausata, E. Jansen, B. Risebrobakken & R. J. Telford (2009) Holocene trends in the foraminifer record from the Norwegian Sea and the North Atlantic Ocean. *Clim. Past Discuss.,* 5**,** 2081-2113.

Andersen, C., N. Koc & M. Moros (2004) A highly unstable Holocene climate in the subpolar North Atlantic: evidence from diatoms. *Quaternary Science Reviews,* 23**,** 2155-2166.

Aure, J., and Ø. Strand (2001), Hydrografiske normaler og langtidsvariasjoner i norske kystfarvann mellom 1936 og 2000, *Fisken og havet, 13*, 1-24.

Austin, W. E. N. and Salomonsen, G. in prep. Oxygen isotope mixing line along the coast of NW Europe: implications for paleoclimatic studies.

Bakke, J., O. Lie, E. Heegaard, T. Dokken, G. H. Haug, H. H. Birks, P. Dulski & T. Nilsen (2009) Rapid oceanic and atmospheric changes during the Younger Dryas cold period. *Nature Geosci,* 2**,** 202-205.

Bakke, J., S. O. Dahl, Ø. Paasche, J. Riis Simonsen, B. Kvisvik, K. Bakke & A. Nesje (2010) A complete record of Holocene glacier variability at Austre Okstindbreen, northern Norway: an integrated approach. *Quaternary Science Reviews,* 29**,** 1246-1262.

Barker, S., M. Greaves, and H. Elderfield (2003), A study of cleaning procedures used for foraminiferal Mg/Ca paleothermometry, *Geochem. Geophys. Geosyst., 4*, doi. 10.1029/2003gc000559.

Bauch, H. A., H. Erlenkeuser, R. F. Spielhagen, U. Struck, J. Matthiessen, J. Thiede & J. Heinemeier (2001) A multiproxy reconstruction of the evolution of deep and surface waters in the subarctic Nordic seas over the last 30,000 yr. *Quaternary Science Reviews,* 20**,** 659-678.

Beer, J. (2001) Ice core data on climate and cosmic ray changes. *in: J. Kirkby and S. Mele (eds.), Ion-Aerosol-Cloud Interactions, Proc. Workshop on Ion-Aerosol-Cloud Interactions, CERN Yellow Report, 2001(007),* ISSN 0007-8328, ISBN 92-9083-191-0, CERN, Geneva, Switzerland**,** 3-11.

Berger, A., and M. F. Loutre (1991), Insolation values for the climate of the last 10 million years, *Quaternary Sciences Review, 10*, 297–317.

Birgel, D. & H. C. Hass (2004) Oceanic and atmospheric variations during the last deglaciation in the Fram Strait (Arctic Ocean): a coupled high-resolution organic-geochemical and sedimentological study. *Quaternary Science Reviews,* 23**,** 29-47.

Birks, C. J. A. & N. Koç (2002) A high-resolution diatom record of late-Quaternary sea-surface temperatures and oceanographic conditions from the eastern Norwegian Sea. *Boreas,* 31**,** 323 - 344.

Bond, G., W. Showers, M. Cheseby, R. Lotti, P. Almasi, P. deMenocal, P. Priore, H. Cullen, I. Hajdas & G. Bonani (1997) A Pervasive Millennial-Scale Cycle in North Atlantic Holocene and Glacial Climates. *Science,* 278**,** 1257-1266.

Bond, G., B. Kromer, J. Beer, R. Muscheler, M. N. Evans, W. Showers, S. Hoffmann, R. Lotti-Bond, I. Hajdas & G. Bonani (2001) Persistent Solar Influence on North Atlantic Climate During the Holocene. *Science,* 294**,** 2130-2136.

Bondevik, S., Birks, H. H., Gulliksen, S., and Mangerud, J. (1999). Late Weichselian Marine ^{14}C Reservoir Ages at the Western Coast of Norway. Quaternary Research 52, 104-114.

Bondevik, S., Mangerud, J., Birks, H. H., Gulliksen, S., and Reimer, P. (2006). Changes in North Atlantic Radiocarbon Reservoir Ages during the Allerød and Younger Dryas. Sceince 312, 1514-1517.

Bourke, R. H., A. M. Weigel, and R. G. Paquette (1988), The Westward Turning Branch of the West Spitsbergen Current, J. Geophys. Res., 93, 14065-14077.

Boyle, E. A. (1983), Manganese carbonate overgrowths on foraminifera tests, *Geochimica et Cosmochimica Acta 47*, 1815–1819.

Boyle, E. A., and Keigwin, L. D. (1985). Comparison of Atlantic and Pacific paleochemical records for the last 215,000 years: changes in deep ocean circulation and chemical inventories. Earth and Planetary Science Letters 76, 135-150.

Boyle, E. A., and Rosenthal, Y. (1996). Chemical hydrography of the South Atlantic during the Last Glacial Maximum: Cd and d13C, in The South Atlantic: Present and Past Circulation. edited by G. Wefer et al. Springer-Verlag, New York, 423 –443.

Carstens, J., D. Hebbeln & G. Wefer (1997) Distribution of planktic foraminifera at the ice margin in the Arctic (Fram Strait). *Marine Micropaleontology,* 29**,** 257-269.

Chaudhuri, P., and S. Marron (1999), SiZer for exploration of sturctures in curves, *Journal of the Amerikan Statistical Association, 94*, 807-823.

Dolven, J. K., G. Cortese & K. R. Bjørklund (2002) A high-resolution radiolarian-derived paleotemperature record for the Late Pleistocene-Holocene in the Norwegian Sea. *Paleoceanography,* 17**,** 1072. doi.10.1029/2002pa000780.

Ebbesen, H., and M. Hald (2004), Unstable Younger Dryas climate in the northeast North Atlantic, *Geology, 32*(8), 673-676.

Ebbesen, H., M. Hald & T. H. Eplet (2007) Late glacial and early Holocene climatic oscillations on the western Svalbard margin, European Arctic. *Quarternary Science Reviews,* 26**,** 1999-2011.

Eilertsen, R., G. D. Corner & O. Aasheim (2005) Deglaciation chronology and glaciomarine successions in the Malangen-Målselv area, northern Norway. *Boreas,* 34**,** 233 - 251.

Elderfield, H. & G. M. Ganssen (2000) Past temperature and $d^{18}O$ of surface ocean waters inferred from foraminiferal Mg/Ca ratios. *Nature,* 405**,** 442–445.

Elderfield, H., Vautravers, M., and Cooper, M. (2002). The relationship between shell size and Mg/Ca, Sr/Ca, $\delta^{18}O$, and $\delta^{13}C$ of species of planktonic foraminifera. Geochem. Geophys. Geosyst. 3(8). Doi:10.1029/2001gc000194

Elverhøi, A., E. S. Andersen, T. Dokken, D. Hebbeln, R. Spielhagen, J. I. Svendsen, M. Sorflaten, A. Rornes, M. Hald & C. F. Forsberg (1995) The Growth and Decay of the Late Weichselian Ice Sheet in Western Svalbard and Adjacent Areas Based on Provenance Studies of Marine Sediments. *Quaternary Research,* 44**,** 303-316.

Fairbanks, R. G. (1989), A 17,000-year glacio-eustatic sea level record : influence of glacial melting rates on the Younger Dryas event and deep-ocean circulation, *Nature (London), 342*, 637-642.

Farmer, E. J., M. R. Chapman & J. E. Andrews (2008) Centennial-scale Holocene North Atlantic surface temperatures from Mg/Ca ratios in Globigerina bulloides. *Geochem. Geophys. Geosyst.,* 9**,** doi.10.1029/2008GC002199.

Furevik, T., C. Mauritzen & R. Ingvaldsen (2007) The Flow of Atlantic Water to the Nordic Seas and Arctic Ocean. *in Arctic-Alpine Ecosystems and People in a Changing Environment (J.B. Ørbæk, R Kallenborn, I Tombre, E Nøst Hegseth, S Falk-Petersen, A.H. Hoel, Eds.), Springer Verlag***,** 123-146.

Giraudeau, J., A. E. Jennings & J. T. Andrews (2004) Timing and mechanisms of surface and intermediate water circulation changes in the Nordic Seas over the last 10,000 cal years: a view from the North Iceland shelf. *Quaternary Science Reviews,* 23**,** 2127-2139.

Giraudeau, J., (in prep) EPOC (University Bordeaux 1/CNRS) within the framework of an ongoing IFM-GEOMAR / EPOC collaboration

Grönvold, K., N. Oskarsson, S. J. Johnsen, H. B. Clausen, C. U. Hammer, G. Bond & E. Bard (1995) Ash layers from Iceland in the Greenland GRIP ice core correlated with oceanic and land sediments. *Earth and Planetary Science Letters,* 135**,** 149–155.

Hagen, S. (1995), Watermass Characteristics and Climate in the Nordic Sea During the Last 10,200 Years, *Master Thesis, University of Tromsø*, pp 114.

Hald, M. & R. Aspeli (1997) Rapid climatic shifts of the nothern Norwegian Sea during the last deglaciation and the Holocene. *Boreas,* 26**,** 15-28.

Hald, M. & S. Hagen (1998) Early preboreal cooling in the Nordic Sea region triggered by meltwater *Geology* 26**,** 615-618.

Hald, M., C. Andersson, H. Ebbesen, E. Jansen, D. Klitgaard-Kristensen, B. Risebrobakken, G. R. Salomonsen, H. P. Sejrup, M. Sarnthein & R. Telford (2007) Variations in temperature and extent of Atlantic Water in the northern North Atlantic during the Holocene. *Quaternary Science Reviews,* 26**,** 3423-3440.

Hansen, B. & S. Osterhus (2000) North Atlantic-Nordic Seas exchanges. *Progress In Oceanography,* 45**,** 109-208.

Hopkins, T. S. (1991), The GIN Sea--A synthesis of its physical oceanography and literature review 1972-1985, *Earth-Science Reviews*, *30*(3-4), 175-318.

Hughen, K. A., Baillie, M. G. L., Bard, E., Beck, J. W., Bertrand, C. J. H., Blackwell, P. G., Buck, C. E., Burr, G. S., Cutler, K. B., Damon, P. E., Edwards, R. L., Fairbanks, R. G., Friedrich, M., Guilderson, T. P., Kromer, B., McCormac, G., Manning, S., Ramsey, C. B., Reimer, P. J., Reimer, R. W., Remmele, S., Southon, J. R., Stuiver, M., Talamo, S., Taylor, F. W., van der Plicht, J., and Weyhenmeyer, C. E. (2004). Marine04 marine radiocarbon age calibration, 0-26 cal kyr BP. Radiocarbon 46, 1059-1086.

Hurrell, J. W. (1995) Decadal Trends in the North Atlantic Oscillation Regional Temperatures and Precipitation. *Science,* 269**,** 676-679.

IPCC (2007) Climate Change 2007: The physical science basis. Summary for policymakers, intergovernmental panel on climate change. *Fourth Assessment Report, Geneva, IPCC Secretariat***,** 1–18.

Jansen, E., Andersson, C., Moros, M., Nisancioglu, K. H., Nyland, B. F., and Telford, R. J. 2008: The early to mid-Holocene thermal optimum in the North Atlantic, in: Natural Climate Variability and Global Warming – A Holocene Perspective, edited by: Battarbee, R. W. and Binney, H. A., Wiley-Blackwell, Chichester, 123–137.

Jessen, S. P., T. L. Rasmussen, T. Nielsen & A. Solheim (2010) A new Late Weichselian and Holocene marine chronology for the western Svalbard slope 30,000-0 cal years BP. *Quaternary Science Reviews,* 29**,** 1301-1312.

Johannessen, T., E. Jansen, A. Flatøy & A. C. Ravalo (1994) The relationship between surface water masses, oceanographic fronts and paleoclimatic proxies in surface sediments of the Greenland, Iceland and Norwegian Seas. *NATO ASI series I,* 17**,** 61-85.

Johnsen, S. J., D. Dahl-Jensen, N. Gundestrup, J. P. Steffensen, H. B. Clausen, H. Miller, V. Masson-Delmotte, A. E. Sveinbjôrnsdottir & J. White (2001) Oxygen isotope and palaeotemperature records from six Greenland ice-core stations: Camp Century, Dye-3, GRIP, GISP2, Renland and NorthGRIP. *Journal of Quaternary Science,* 16**,** 299–307.

Jonkers, L., G.-J. A. Brummer, F. J. C. Peeters, H. M. van Aken & M. F. De Jong (2010) Seasonal stratification, shell flux, and oxygen isotope dynamics of left-coiling N. pachyderma and T. quinqueloba in the western subpolar North Atlantic. *Paleoceanography,* 25**,** PA2204. doi: 10.1029/2009pa001849

Klitgaard-Kristensen, D., H. P. Sejrup & H. Haflidason (2001) The last 18 kyr fluctuations in Norwegian Sea surface conditions and implicationsfor the magnitude of climatic change, evidence from the northern North Sea. *Paleoceanography,* 16**,** 455–467.

Knies, J., M. Hald, H. Ebbesen, U. Mann & C. Vogt (2003) A deglacial—middle Holocene record of biogenic sedimentation and paleoproductivity changes from the northern Norwegian continental shelf. *Paleoceanography,* 18**,** 1096, doi:10.1029/2002PA000872,.

Knudsen, K. L., H. Jiang, E. Jansen, J. EirIksson, J. Heinemeier & M. S. Seidenkrantz (2004) Environmental changes off North Iceland during the deglaciation and the Holocene: foraminifera, diatoms and stable isotopes. *Marine Micropaleontology,* 50**,** 273-305.

Koç Karpuz, N. & E. Jansen (1992) A high-resolution diatom record of the last deglaciation from the SE Norwegian Sea: Documentation of rapid climatic changes. *Paleoceanography,* 7**,** 499– 520.

Koç, N., E. Jansen & H. Haflidason (1993) Paleoceanographic reconstructions of surface ocean conditions in the Greenland, Iceland and Norwegian seas through the last 14 ka based on diatoms. *Quaternary Science Reviews,* 12**,** 115-140.

Kozdon, R., A. Eisenhauer, M. Weinelt, M. Y. Meland, and D. Nürnberg (2009), Reassessing Mg/Ca temperature calibrations of Neogloboquadrina pachyderma (sinistral) using paired δ44/40Ca and Mg/Ca measurements, *Geochemistry Geophysics Geosystems*, *10*, http://dx.doi.org/10.1029/2008GC002169

Kristjánsdóttir, G. B., D. W. Lea, A. E. Jennings, D. K. Pak, and C. Belanger (2007), New spatial Mg/Ca-temperature calibrations for three Arctic, benthic foraminifera and reconstruction of north Iceland shelf temperature for the past 4000 years, *Geochem. Geophys. Geosyst.*, *8*, doi. 10.1029/2006gc001425.

Landvik, J. Y., S. Bondevik, A. Elverhoi, W. Fjeldskaar, J. Mangerud, O. Salvigsen, M. J. Siegert, J.-I. Svendsen & T. O. Vorren (1998) The last glacial maximum of Svalbard and the Barents sea area: ice sheet extent and configuration. *Quaternary Science Reviews,* 17**,** 43-75.

Lear, C. H., Y. Rosenthal, and N. Slowey (2002), Benthic foraminiferal Mg/Ca-paleothermometry: a revised core-top calibration, *Geochimica et Cosmochimica Acta*, *66*(19), 3375-3387.

Mangerud, J., S. T. Andersen, B. E. Berglund, and D. D. Donner (1974), Quaternary stratigraphy of Norden, a proposal for terminology and classification, *Boreas*, *3*, 109-128.

Mangerud, J. & S. Gulliksen (1975) Apparent radiocarbon ages of Recent marine shells from Norway, Spitsbergen, and Arctic Canada. *Quaternary Research* 5**,** 263-273.

Mangerud, J., S. Bondevik, S. Gulliksen, A. K. Hufthammer & T. Høisæter (2006) Marine14 C reservoir ages for 19th century whales and molluscs from the North Atlantic. *Quaternary Science Reviews,* 25**,** 3228-3245.

Manley, T. O. (1995), Branching of Atlantic Water within the Greenland-Spitsbergen passage: An estimate of recirculation, J. Geophys. Res., 100, 20627-20634.

Marchitto, T. M. (2006) Precise multielemental ratios in small foraminiferal samples determined by sector field ICP-MS. *Geochem. Geophys. Geosyst.,* 7**,** doi. 10.1029/2005gc001018.

Marnela, M., B. Rudels, K. A. Olsson, L. G. Anderson, E. Jeansson, D. J. Torres, M.-J. Messias, J. H. Swift, and A. J. Watson (2008), Transports of Nordic Seas water masses and excess SF6 through Fram Strait to the Arctic Ocean, *Progress In Oceanography*, *78*(1), 1-11.

Mayewski, P. A., E. E. Rohling, J. Curt Stager, W. Karlen, K. A. Maasch, L. David Meeker, E. A. Meyerson, F. Gasse, S. van Kreveld, K. Holmgren, J. Lee-Thorp, G. Rosqvist, F. Rack, M. Staubwasser, R. R. Schneider & E. J. Steig (2004) Holocene climate variability. *Quaternary Research,* 62**,** 243-255.

Meland, M. Y., E. Jansen, and H. Elderfield (2005), Constraints on SST estimates for the northern North Atlantic/Nordic Seas during the LGM, *Quaternary Science Reviews*, *24*(7-9), 835-852.

Mikalsen, G., Sejrup, H. P. and Aarseth, I. 2001. Late-Holocene changes in ocean circulation and climate: foraminiferal and isotopic evidence from Sulafjord, western Norway. *The Holocene* 11, 437-446.

Mosby, H. (1968), Surrounding Seas *In: Sømme, A. (Ed.), Geography of Norden. J.W. Cappelens Forlag, Oslo, Norway*, pp. 18-26.

Nesje, A., J. A. Matthews, S. O. Dahl, M. S. Berrisford & C. Andersson (2001) Holocene glacier fluctuations of Flatebreen and winter-precipitation changes in the Jostedalsbreen region, western Norvay, based on glaciolacustrine sediment records *The Holocene,* 11**,** 267-280. doi:10.1191/095968301669980885

Nordby, E., K. S. Tande, H. Svendsen, and D. Slagstad (1999), Oceanography and fluorescence at the shelf break off the north Norwegian coast (69°20'N–70°30'N) during the main productive period in 1994, *Sarsia*(84), 175-189.

Nürnberg, D. (1995), Magnesium in tests of *Neogloboquadrina pachyderma* sinistral from high northern and southern latitudes, *Journal of Foraminiferal Research*, *25*, 350–368.

Oppo, D. W., J. F. McManus & J. L. Cullen (2003) Palaeo-oceanography: Deepwater variability in the Holocene epoch. *Nature,* 422**,** 277-278.

Plassen, L. & T. O. Vorren (2002) Late Weichselian and Holocene sediment flux and sedimentation rates in Andfjord and Vågsfjord, north Norway. *Journal of Quaternary Science,* 17**,** 1-20.

Poole, D. (1994) Neogene and Quaternary paleoenvironments in the Norwegian Saes shelf: Stable isotope fractionation in recent benthic foraminifera from the Barents and Kara Seas. *PhD thesis, University of Tromsø, Norway***,** 51pp.

Rasmussen, S. O., K. K. Andersen, A. M. Svensson, J. P. Steffensen, B. M. Vinther, H. B. Clausen, M.-L. Siggaard-Andersen, S. J. Johnsen, L. B. Larsen, D. Dahl-Jensen, R. R. Bigler, M. , H. Fischer, K. Goto-Azuma, M. E. Hansson & U. Ruth (2006) A new Greenland ice core chronology for the last glacial termination. *Journal of Geophysical Research,* 111**,** 16 pp. doi:10.1029/2005JD006079

Rasmussen, S. O., Vinther, B. M., Clausen, H. B., and Andersen, K. K. (2007). Early Holocene climate oscillations recorded in three Greenland ice cores. Quaternary Science Reviews 26, 1907-1914.

Rasmussen, T. L., E. Thomsen, M. A. Slubowska, S. Jessen, A. Solheim & N. Koc (2007) Paleoceanographic evolution of the SW Svalbard margin (76^0N) since 20,000 ^{14}C yr BP. *Quaternary Research,* 67**,** 100-114.

Rasmussen, T. L. & E. Thomsen (2010) Holocene temperature and salinity variability of the Atlantic Water inflow to the Nordic seas *Holocene,* 20**,** 1223-1234.

Reimer, P. J., Baillie, M. G. L., Bard, E., Bayliss, A., Beck, J. W., Bertrand, C. J. H., Blackwell, P. G., Buck, C. E., Burr, G. S., Cutler, K. B., Damon, P. E., Edwards, R. L., Fairbanks, R. G., Friedrich, M., Guilderson, T. P., Hogg, A. G., Hughen, K. A., Kromer, B., McCormac, F. G., Manning, S. W., Ramsey, C. B., Reimer, R. W., Remmele, S., Southon, J. R., Stuiver, M., Talamo, S., Taylor, F. W., van der Plicht, J., and Weyhenmeyer, C. E. (2005). IntCal04 Terrestrial radiocarbon age calibration, 26 - 0 ka BP. Radiocarbon 46, 1029-1058.

Reimer, P. J., Baillie, M. G. L., Bard, E., Bayliss, A., Beck, J. W., Blackwell, P. G., Bronk Ramsey, C., Buck, C. E., Burr, G. S., Edwards, R. L., Friedrich, M., Grootes, P. M., Guilderson, T. P., Hajdas, I., Heaton, T. J., Hogg, A. G., Hughen, K. A., Kaiser, K. F., Kromer, B., McCormac, F. G., Manning, S. W., Reimer, R. W., Richards, D. A., Southon, J. R., Talamo, S., Turney, C. S. M., van der Plicht, J., and Weyhenmeyer, C. E. (2009). IntCal09 and Marine09 Radiocarbon Age Calibration Curves, 0–50,000 Years cal BP. Radiocarbon 51, 1111–1150.

Risebrobakken, B., E. Jansen, C. Andersson, E. Mjelde & K. Hevrøy (2003) A high-resolution study of Holocene paleoclimatic and paleoceanographic changes in the Nordic Seas. *Paleoceanography,* 18**,** 1017-1034.

Rudels, B., G. Björk, J. Nilsson, P. Winsor, I. Lake, and C. Nohr (2005), The interaction between waters from the Arctic Ocean and the Nordic Seas north of Fram Strait and along the East Greenland Current: results from the Arctic Ocean-02 Oden expedition, Journal of Marine Systems, 55(1-2), 1-30.

Rørvik, K. L., M. Hald, K. Husum, H. B. Johannessen & T. M. Marchitto (submitted) Holocene paleoceanography in the NE Nordic seas based *Cassidulina neoteretis* Mg/Ca and $d^{18}O_c$ records from the Malangen fjord, North Norway. *Holocene*.

Sarnthein, M., S. Van Kreveld, H. Erlenkeuser, P. M. Grootes, M. Kucera, U. Pflaumann & M. Schulz (2003) Centennial-to-millennial-scale periodicities of Holocene climate and sediment injections off the western Barents shelf, 75°N. *Boreas,* 32**,** 447 - 461.

Schauer, U., H. Loeng, B. Rudels, V. K. Ozhigin, and W. Dieck (2002), Atlantic Water flow through the Barents and Kara Seas, Deep Sea Research Part I: Oceanographic Research Papers, 49(12), 2281-2298.

Schauer, U., E. Fahrbach, S. Østerhus, and G. Rohardt (2004), Arctic warming through the Fram Strait: Oceanic heat transport from 3 years of measurements, Journal of Geophysical Research, 109, C06026, doi:06010.01029/02003JC001823.

Seppä, H., G. M. MacDonald, H. J. B. Birks, B. R. Gervais & J. A. Snyder (2008) Late-Quaternary summer temperature changes in the northern-European tree-line region. *Quaternary Research,* 69**,** 404-412.

Shackleton, N. J. (1974) Attainment ofisotopic equilibrium between ocean water and the benthonic foraminifera genus Uvigerina: isotopic changes in the ocean during the last glacial. *Centre National de la Recherche Scientifique Colleagues Internationeau,* 219**,** 203-209.

Simstich, J., M. Sarnthein, and H. Erlenkeuser (2003), Paired delta O-18 signals of Neogloboquadrina pachyderma (s) and Turborotalita quinqueloba show thermal stratification structure in Nordic Seas, *Marine Micropaleontology 48*(1-2), 107-125.

Ślubowska-Woldengen, M., N. Koç, T. L. Rasmussen & D. Klitgaard-Kristensen (2005) Changes in the flow of Atlantic water into the Arctic Ocean since the last deglaciation: Evidence from the northern Svalbard continental margin, 80°N. *Paleoceanography,* 20**,** PA001141.doi: 10.1029/2005PA001141

Ślubowska-Woldengen, M., N. Koç, T. L. Rasmussen, D. Klitgaard-Kristensen, M. Hald, and A. E. Jennings (2008), Time-slice reconstructions of ocean circulation changes on the continental shelf in the Nordic and Barents Seas during the last 16,000 cal yr B.P., *Quaternary Science Reviews*, *27*(15-16), 1476-1492.

Spielhagen, R. F., K. Werner, S. A. Sørensen, K. Zamelczyk, E. Kandiano, G. Budeus, K. Husum, T. M. Marchitto & M. Hald (2011) Enhanced Modern Heat Transfer to the Arctic by Warm Atlantic Water. *SCIENCE,* 331**,** 450-453.

Steffensen, J. P., Andersen, K. K., Bigler, M., Clausen, H. B., Dahl-Jensen, D., Fischer, H., Goto-Azuma, K., Hansson, M., Johnsen, S. J., Jouzel, J., Masson-Delmotte, V., Popp, T., Rasmussen, S. O., Rothlisberger, R., Ruth, U., Stauffer, B., Siggaard-Andersen, M.-L., Sveinbjornsdottir, A. E., Svensson, A., and White, J. W. C. (2008). High-Resolution Greenland Ice Core Data Show Abrupt Climate Change Happens in Few Years. Science 321, 680-684.

Steinhilber, F., J. Beer & C. Fröhlich (2009) Total solar irradiance during the Holocene. *Geophys. Res. Lett.,* 36**,** doi.10.1029/2009gl040142.

Stuiver, M., Reimer, P. J., and Reimer, R. W. 2005. CALIB 6.0. [WWW program and documentation].

Teller, J. T., Leverington, D. W., and Mann, J. D. (2002). Freshwater outbursts to the oceans from glacial Lake Agassiz and their role in climate change during the last deglaciation. Quaternary Science Reviews 21, 879–887.

Thornalley, D. J. R., H. Elderfield & I. N. McCave (2010) Intermediate and deep water paleoceanography of the northern North Atlantic over the past 21,000 years. *Paleoceanography,* 25**,** PA1211. doi. 10.1029/2009pa001833.

Vinther, B. M., H. B. Clausen, S. J. Johnsen, S. O. Rasmussen, K. K. Andersen, S. L. Buchardt, D. Dahl-Jensen, I. K. Seierstad, M. L. Siggaard-Andersen, J. P. Steffensen, A. Svensson, J. Olsen & J. Heinemeier (2006) A synchronized dating of three Greenland ice cores throughout the Holocene. *Journal of Geophysical Research,* 111**,** D13102. doi:10.1029/2005JD006921

Volkmann, R. (2000) Planktic foreminifers in the outer Laptev Sea and the Fram Strait - Modern distribution and ecology. *Journal of Foraminiferal Research,* 30**,** 157-176.

Vorren, T. O., M. Edvardsen, M. Hald & E. Thomsen (1983) Deglaciation of the Continental Shelf off Southern Troms, North Norway. *Norgens Geologiske Undersøgelse,* 380**,** 173-187.

Vorren, K. D., and Moe, D. (1986). The early Holocene climate and sea-level change in Lofoten and Vesterålen, north. Norway. Nor. Geolog. Tidsskr. 66, 135-143.

Vorren, T. O. & L. Plassen (2002) Deglaciation and palaeoclimate of the Andfjord-Vagsfjord area, North Norway. *Boreas,* 31**,** 97-125.

Walczowski, W., J. Piechura, R. Osinski, and P. Wieczorek (2005), The West Spitsbergen Current volume and heat transport from synoptic observations in summer, Deep Sea Research Part I: Oceanographic Research Papers, 52(8), 1374-1391.

Walker, M., Johnsen, S., Rasmussen, S. O., Popp, T., Steffensen, J.-P., Gibbard, P., Hoek, W., Lowe, J., Andrews, J., Björck, S., C. Cwynar, L., Hughen, K., Kershaw, P., Kromer, B., Litt, T., J. Lowe, D., Nakagawa, T., Newnham, R., and Schwander, J. (2009). Formal definition and dating of the GSSP (Global Stratotype Section and Point) for the base of the Holocene using the Greenland NGRIP ice core, and selected auxiliary records. Journal of Quaternary Science 24, 3-17.

Figure captions

Table 1. Core location, water depth, length, geographical area and new proxies and reference of previous works.

Table 2A-C. Radiocarbon datings, Vedde Ash horizon and calendar year calibrations for the proxy records in Andfjorden: (A) T79-51/2, (B) JM99-1200 and the Eastern Fram Strait (C) MSM5/5-712. A standard reservoir correction of 400 years with an additional reservoir correction ΔR was used. Andfjorden: ΔR=64±35; YD ΔR=200±50. Eastern Fram Strait: ΔR=151±51.

Figure 1. (A) Map of northern North Atlantic and adjoining seas showing major currents systems, oceanic fronts and sea ice limits modified from Mosby (1968), Hopkins (1991) and Marnela et al. (2008). VP=Vøring Plateau. (B) Zoom in on the Fram Strait with core site. (C) Zoom in on Andfjorden with core sites. AO=Arctic Ocean, BS=Barents Sea.

Figure 2. Conductivity, temperature, and depth (CTD). (A) Andfjorden, October 1999. (B) Eastern Fram Strait, August 2007. Solid line = salinity. Dashed line = temperature.

Figure 3. Age model and bulk sediment accumulation rate (cm/kyr) of cores (A) T79-51/2 + JM99-1200 and (B) MSM5/5-712. The age models are developed by linear interpolation between the calibrated radiocarbon dated levels (Points) and Vedde Ash layer (Diamond). Error bars depict 2σ standard deviation on calibrated ages.

Figure 4. Trace metal concentrations and stable isotope measurements versus calibrated age and depth in cores T79-51/2 (black lines) and JM99-1200 (grey lines). (A) $CaCO_3$ recovery (µg). Broken line= minimum recovery level for sample omittance (5µg) (Marchitto, 2006). (B) Mg/Ca concentration (mmol/mol). Crosses mark omitted data points. Filled circle shows the average reproducibility of sample splits (±0.088 mmol/mol). (C, D, E) Mn/Ca, Fe/Ca and Al/Ca concentrations (µmol/mol). Broken lines = threshold level of possible contamination (100 µmol/mol) (Barker et al., 2003) (see text for discussion). (F) $\delta^{18}O$ measured on *C. laevigata* in T79-51/2 (present study) and on *C. reniforme* in JM99-1200 (Ebbesen and Hald, 2004). (G) $\delta^{13}C$ measured on *C. laevigata* in T79-51/2 (present study) and on *C. reniforme* in JM99-1200 (Ebbesen and Hald, 2004). Diamonds on X-axis indicate radiocarbon dated levels.

Figure 5. Trace metal concentrations versus calibrated age and depth in core MSM05/5-712-2. (A) $CaCO_3$ recovery (µg). Broken line= minimum recovery level for sample omittance (5µg) (Marchitto, 2006). (B) Mg/Ca concentration (mmol/mol). Thin line = raw data. Thick line = 5-point running mean. Crosses mark omitted data points. Filled

circle shows the average reproducibility of sample splits (±0.044 mmol/mol). (C, D, E) Mn/Ca, Fe/Ca and Al/Ca concentrations (µmol/mol). Broken lines = threshold level of possible contamination (100 µmol/mol) (Barker et al., 2003). Diamonds on X-axis indicate radiocarbon dated levels.

Figure 6. Correlation between Mg/Ca and contamination indicator concentrations. (A) Individual Mg/Ca vs. Fe/Ca, Al/Ca and Mn/Ca and regressions between records in cores T79-51/2 + JM99-1200. (B) Individual Mg/Ca vs. Fe/Ca and Mn/Ca in MSM05/5-712-2 and regressions between records.

Figure 7. Bottom and surface water temperatures and bottom water salinity versus calibrated age and depth. (A) (Left) $BWT_{Isotope}$ calculated from stable oxygen isotopes assuming a constant salinity of 34.5 (Mikalsen et al., 2001), using the equation of Shackleton (1974). (Right) $\delta^{18}O$ measured on *C. laevigata* in T79-51/2 (B) $BWT_{Mg/Ca}$ calculated from Mg/Ca values using Eq.1 (Kristjánsdóttir et al., 2007) (Standard Error ±1.1°C). (C) Relative salinity changes. Seawater $\delta^{18}O_{Bottom\ water,\ vs.V\text{-}SMOW}$ (‰) inferred from the foraminiferal $\delta^{18}O$ and Mg/Ca. (D) $SST_{Mg/Ca}$ calculated from Mg/Ca values using Eq.2 (Kozdon et al., 2009) (E) Black line = positive NAO index, No line = negative NAO index (Nesje et al., 2001). (F) Boxes showing approximate periods of increased drift ice and IRD production (Bond et al., 1997). (G) Total solar irradiance. Thick line = 59-point running mean (300 years) (Steinhilber et al., 2009). (H) Benthic $\delta^{13}C$ values. Proxy for North Atlantic Deep Water formation (Oppo et al., 2003). Thick line = 5-point running mean. (I) June insolation at 70 and 80°N (Berger and Loutre, 1991). (J) NGRIP $\delta^{18}O$ (‰) values (Vinther et al., 2006; Rasmussen et al., 2006).

Figure 8. SiZer analysis of proxy data from cores T79-51/2 (1), JM99-1200 (2) and MSM5/5-712-2 (3). (A) (1) SiZer of Mg/Ca-ratios (*M. barleanus*). (B) (1) SiZer of $\delta^{18}O$ values (*C. laevigata*). (C) (1) TwoSiZer of $\delta^{18}O$ - Mg/Ca. (D) (1+2) SiZer of $BWT_{Mg/Ca}$. (E) (3) SiZer of $SST_{Mg/Ca}$ (linear formula). (F) TwoSiZer of $BWT_{Mg/Ca}$ (1+2) - $SST_{Mg/Ca}$ (3). In the top panel of each SiZer figure a family of smooths (h-values) is given. The dots show all data and the thin lines show smooths obtained from various values of h. In the lower panel a SiZer map shows at what given time significant increase (red), decrease (blue), no change (purple) or where there are too few observations (grey). In the top panel of each twoSiZer figure the two proxy records subtracted from each other are shown. In the lower panel a twoSiZer map shows at what given time significant relative changes between the two proxy- records occur. Color codes are the same as for the SiZer.

Table 1

Core id	Latitude	Longitude	Water depth (m)	Core length (m)	Location	New proxies	References
T79-51/2	69°18.00´N	16°23.00´E	505	3.45	North Norwegian margin (Andfjorden)	Mg/Ca Isotopes	Hald et al. (1996) Hald and Hagen, 1998
JM99-1200	69°15.95'N	16°25.09'E	476	11.12	North Norwegian margin (Andfjorden)	Mg/Ca	Ebbesen and Hald, 2004
MSM05/5-712-2	78˚54.94'N	06˚46.03'E	1487	9.5	West Spitsbergen slope	Mg/Ca	Present study

Table 2A

Core id	Lab. code	Depth range (cm)	Material	^{14}C age	Calibrated age ± 2σ	2 σ max cal. age (cal. age intercepts) 2 σ min cal. age	Reservoir age (R=400 + ΔR)	References
T 79-51/2	TUa-1119	0-3	*Yoldiella* sp.	905±65	437±132	304 (437) 569	464±35	Hald and Hagen (1998)
T 79-51/2	TUa-948	59-61	*Yoldiella* sp.	4195±65	4190±211	3979 (4190) 4400	464±35	Hald and Hagen (1998)
T 79-51/2	TUa-1120	97-99	*Bathyarca pectun*	9000±80	-----	Excluded, reversal	464±35	Hald and Hagen (1998)
T 79-51/2	TUa-949	133-135	*Yoldiella* sp.	8570±65	9163±192	8971 (9163) 9354	464±35	Hald and Hagen (1998)
T 79-51/2	TUa-950	147-149	*Yoldiella* sp.	9334±100	10044±313	9731 (10044) 10356	464±35	Hald and Hagen (1998)
T 79-51/2	TUa-951	225-227	*Yoldiella* sp.	9995±95	10863±265	10598 (10863) 11127	464±35	Hald and Hagen (1998)
T 79-51/2	TUa-952	251-253	*Yoldiella lenticula*	10405±95	11279 ±377	10902 (11279) 11656	600±50	Hald and Hagen (1998)
T 79-51/2	TUa-1121	287-289	*Yoldiella* sp.	10560±90	11467 ±296	11171 (11467) 11763	600±50	Hald and Hagen (1998)
T 79-51/2	NSRL-2057	317-319	*Nuculana* sp.	10620±70	11550±321	11229 (11550) 11870	600±50	Hald and Hagen (1998)

Table 2B

Core id	Lab. code	Depth range (cm)	Material	^{14}C age	Calibrated age ± 2σ	2 σ max cal. age (cal. age intercepts) 2 σ min cal. age	Reservoir age (R=400 + ΔR)	References
JM99-1200		436.5	Tephra	Vedde ash	11982			Ebbesen and Hald (2004)
JM99-1200	Tua-3730	457.5	shell fragments	11165±90	12590±229	12361(12590)12819	464±35	Ebbesen and Hald (2004)
JM99-1200	TUa-2922	511	*Nuculana pernula*	11460±85	12880±217	12663(12880)13097	464±35	Ebbesen and Hald (2004)
JM99-1200	TUa-2923	655.5	*Bathuarca glacialis*	11830±85	13256±171	13085(13256)13427	464±35	Ebbesen and Hald (2004)
JM99-1200	Tua-2924	723.5	*Bathuarca glacialis*	12160±80	13553±171	13347(13553)13758	464±35	Ebbesen and Hald (2004)
JM99-1200	KIA-11109	788	*Bathuarca glacialis*	12425±55	13815±178	13637(13815)13992	464±35	Ebbesen and Hald (2004)
JM99-1200	Tua-3030	855	*Bathuarca glacialis*	12575±100	13973±273	13700(13973)14246	464±35	Ebbesen and Hald (2004)

Table 2C

Core id	Lab. code	Depth range (cm)	Material	^{14}C age	Calibrated age ± 2σ	2 σ max cal. age (cal. age intercepts) 2 σ min cal. age	Reservoir age (R=400 + ΔR)	References
MSM5/5-712-2		20 -22	*N. pachyderma*	1570±25	972±141	831(972)1113	551±51	Werner and Spielhagen (in prep)
MSM5/5-712-2		60-61	*N. pachyderma*	3365±30	3029±175	2854(3029)3203	551±51	Giraudeau (in prep)
MSM5/5-712-2		94-95	*N. pachyderma*	4915±30	5041±189	4852(5041)5230	551±51	Giraudeau (in prep)
MSM5/5-712-2		138.5-139.5	*N. pachyderma*	6440±30	6756±151	6605(6756)6906	551±51	Giraudeau (in prep)
MSM5/5-712-2		168.5-169.5	*N. pachyderma*	7305 ±35	7630±126	7504(7630) 7756	551±51	Werner and Spielhagen (in prep)
MSM5/5-712-2		191.5-192.5	*N. pachyderma*	7815±45	8133±157	7976 (8133) 8290	551±51	Werner and Spielhagen (in prep)
MSM5/5-712-2	Poz-30723	214-215	*N. pachyderma*	8362±45	8749 ±209	8540 (8749) 8958	551±51	Aagaard et al. (in prep)
MSM5/5-712-2	KIA 37423	280-281	*N. pachyderma*	9220±50	9797±252	9551 (9797) 10042	551±51	Aagaard et al. (in prep)
MSM5/5-712-2	Poz-30725	322-323	*N. pachyderma*	9580±47	10310 ±158	10152 (10310) 10468	551±51	Aagaard et al. (in prep)
MSM5/5-712-2	Poz-30726	428-431	*N. pachyderma*	12358±63	13629±197	13432 (13629) 13826	551±51	Aagaard et al. (in prep)

Figure 1

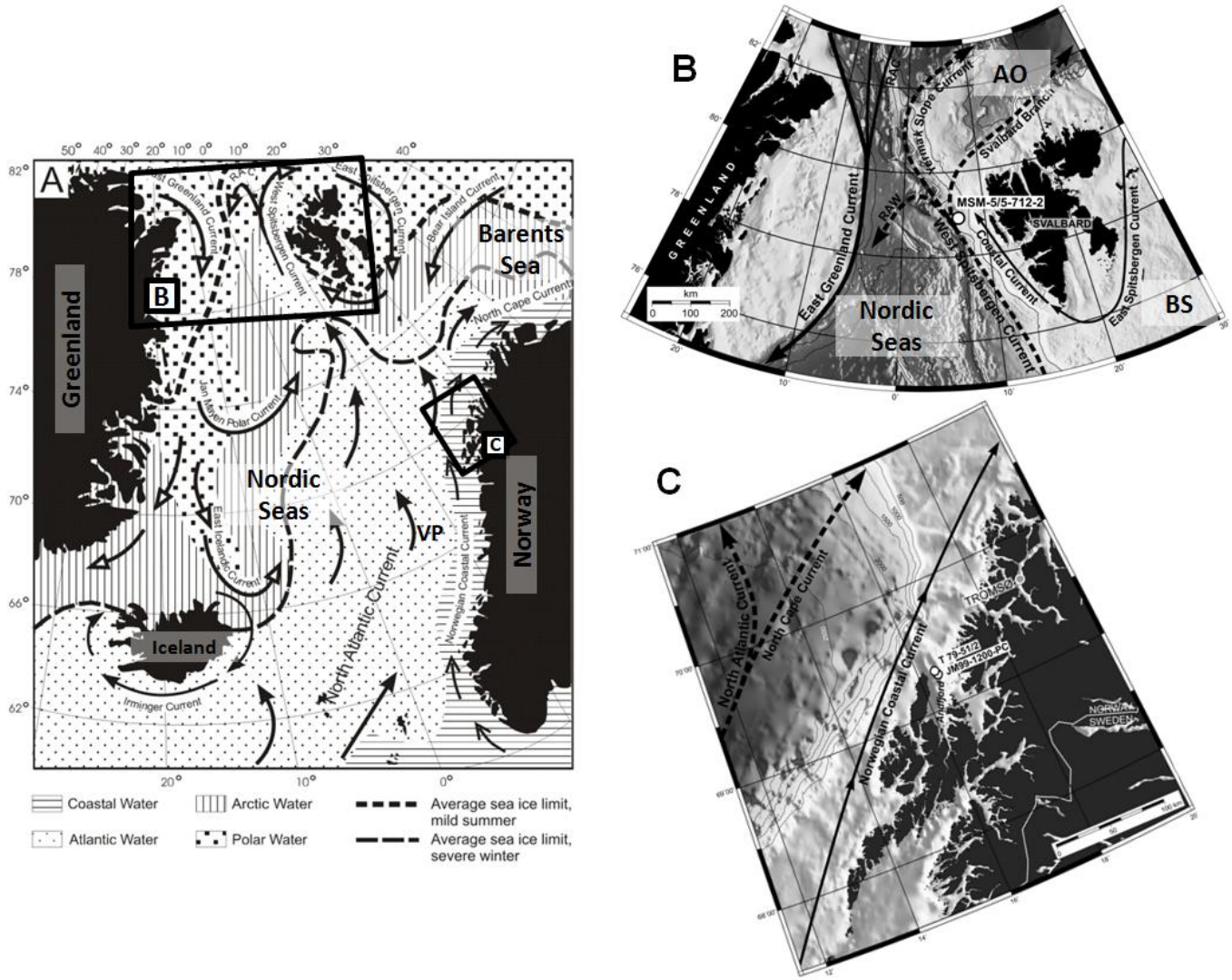
A
B
C
Greenland
Iceland
Norway
Barents Sea
Nordic Seas
VP
AO
BS
East Greenland Current
West Spitsbergen Current
North Atlantic Current
North Cape Current
Norwegian Coastal Current
Irminger Current
Jan Mayen Polar Current
East Icelandic Current
Bear Island Current
East Spitsbergen Current
Coastal Water
Atlantic Water
Arctic Water
Polar Water
Average sea ice limit, mild summer
Average sea ice limit, severe winter
MSM-5/5-712-2
SVALBARD
TROMSØ
T 79-51/2
JM99-1200-PC

Figure 2

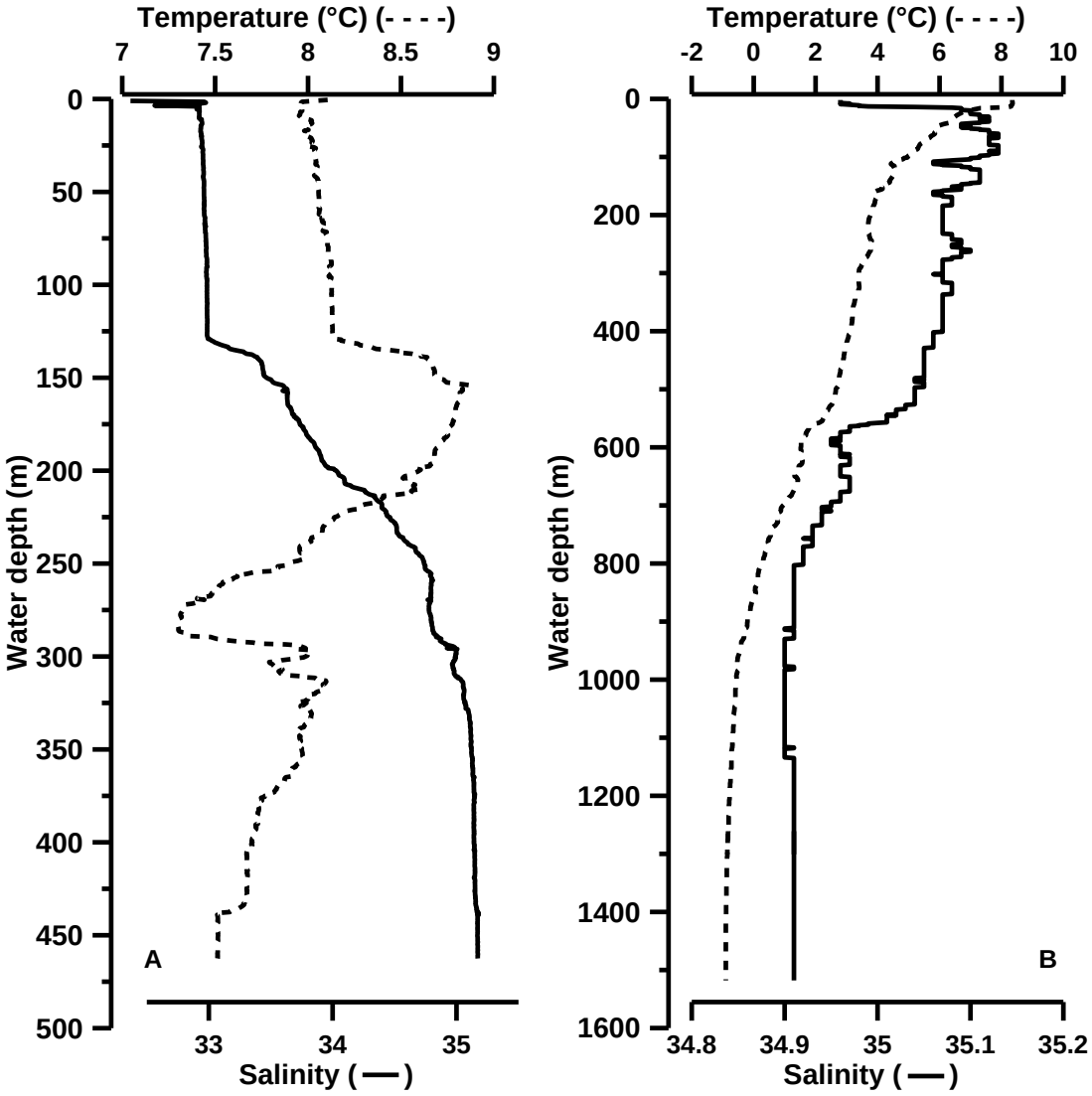
Temperature (°C) (- - - -)
7
7.5
8
8.5
9
0
50
100
150
200
250
300
350
400
450
500
Water depth (m)
A
33
34
35
Salinity (—)
Temperature (°C) (- - - -)
-2
0
2
4
6
8
10
0
200
400
600
800
1000
1200
1400
1600
Water depth (m)
B
34.8
34.9
35
35.1
35.2
Salinity (—)

Figure 3

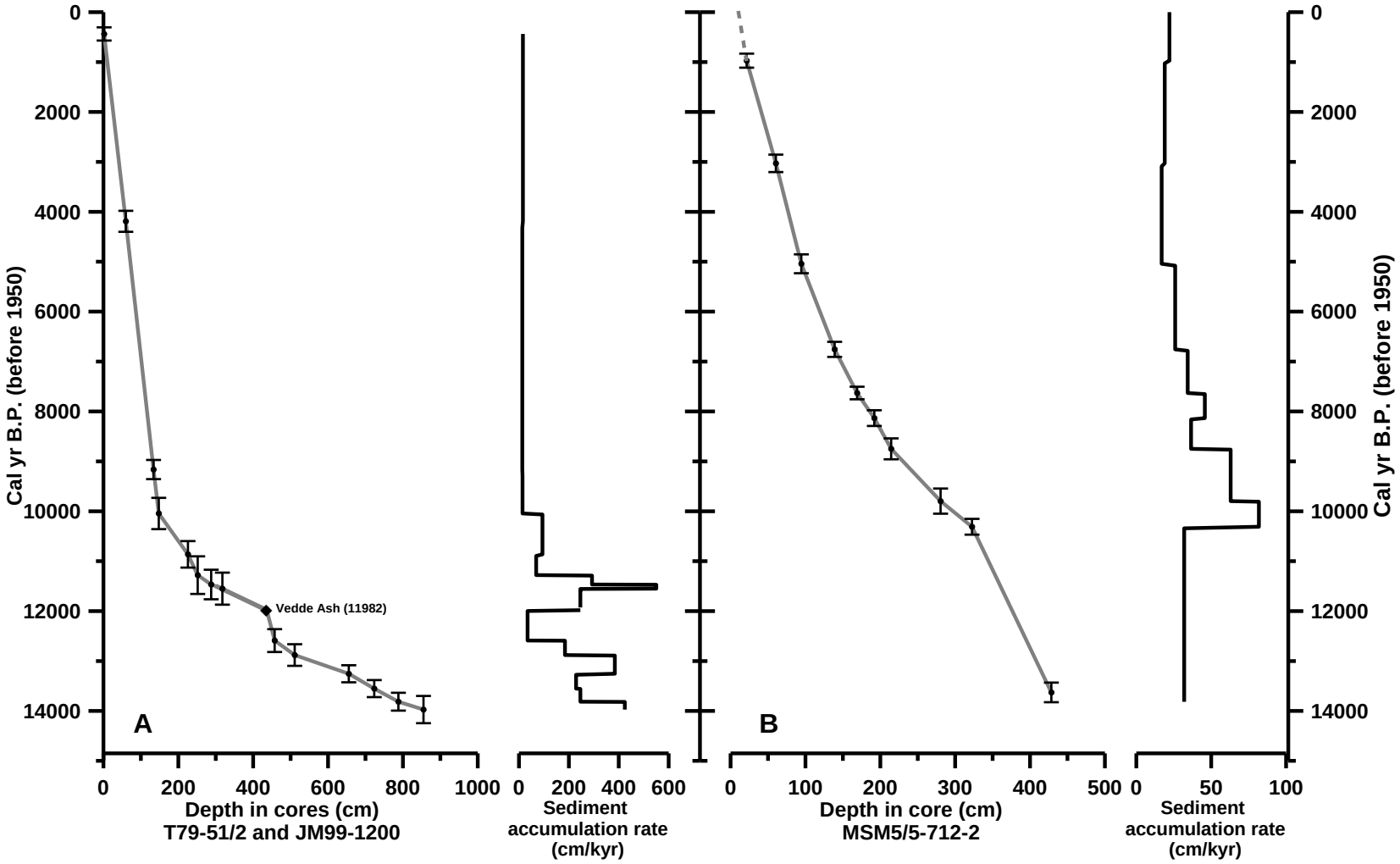
Cal yr B.P. (before 1950)
0
2000
4000
6000
8000
10000
12000
14000
Vedde Ash (11982)
A
0
200
400
600
800
1000
Depth in cores (cm)
T79-51/2 and JM99-1200
0
200
400
600
Sediment
accumulation rate
(cm/kyr)
B
0
100
200
300
400
500
Depth in core (cm)
MSM5/5-712-2
0
50
100
Sediment
accumulation rate
(cm/kyr)
Cal yr B.P. (before 1950)

Figure 4

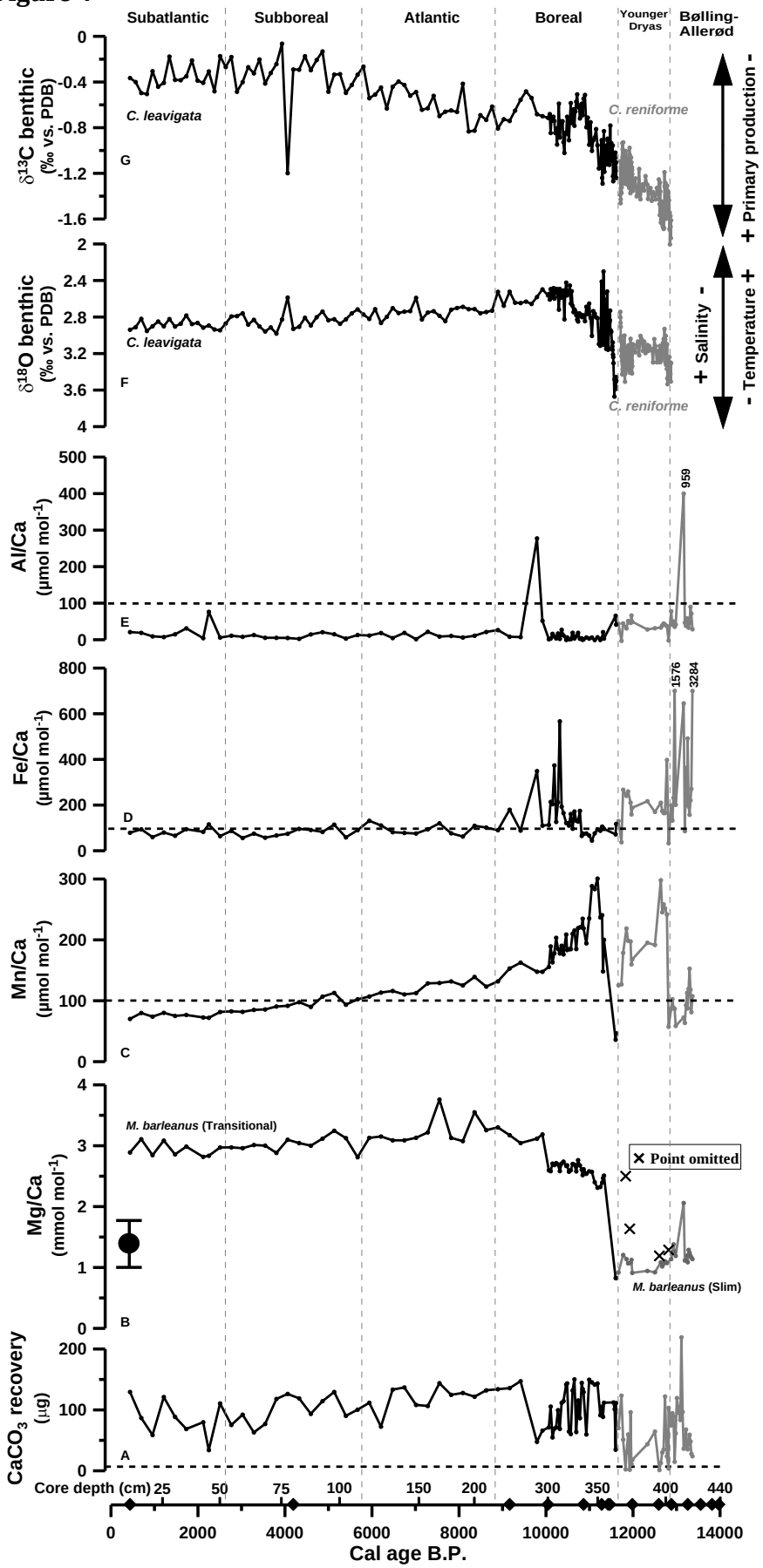
Subatlantic
Subboreal
Atlantic
Boreal
Younger Dryas
Bølling-Allerød
δ13C benthic (‰ vs. PDB)
C. leavigata
C. reniforme
G
+ Primary production -
δ18O benthic (‰ vs. PDB)
C. leavigata
C. reniforme
F
+ Salinity -
- Temperature +
Al/Ca (µmol mol-1)
959
E
Fe/Ca (µmol mol-1)
1576
3284
D
Mn/Ca (µmol mol-1)
C
Mg/Ca (mmol mol-1)
M. barleanus (Transitional)
Point omitted
M. barleanus (Slim)
B
CaCO3 recovery (µg)
A
Core depth (cm)
Cal age B.P.

Figure 5

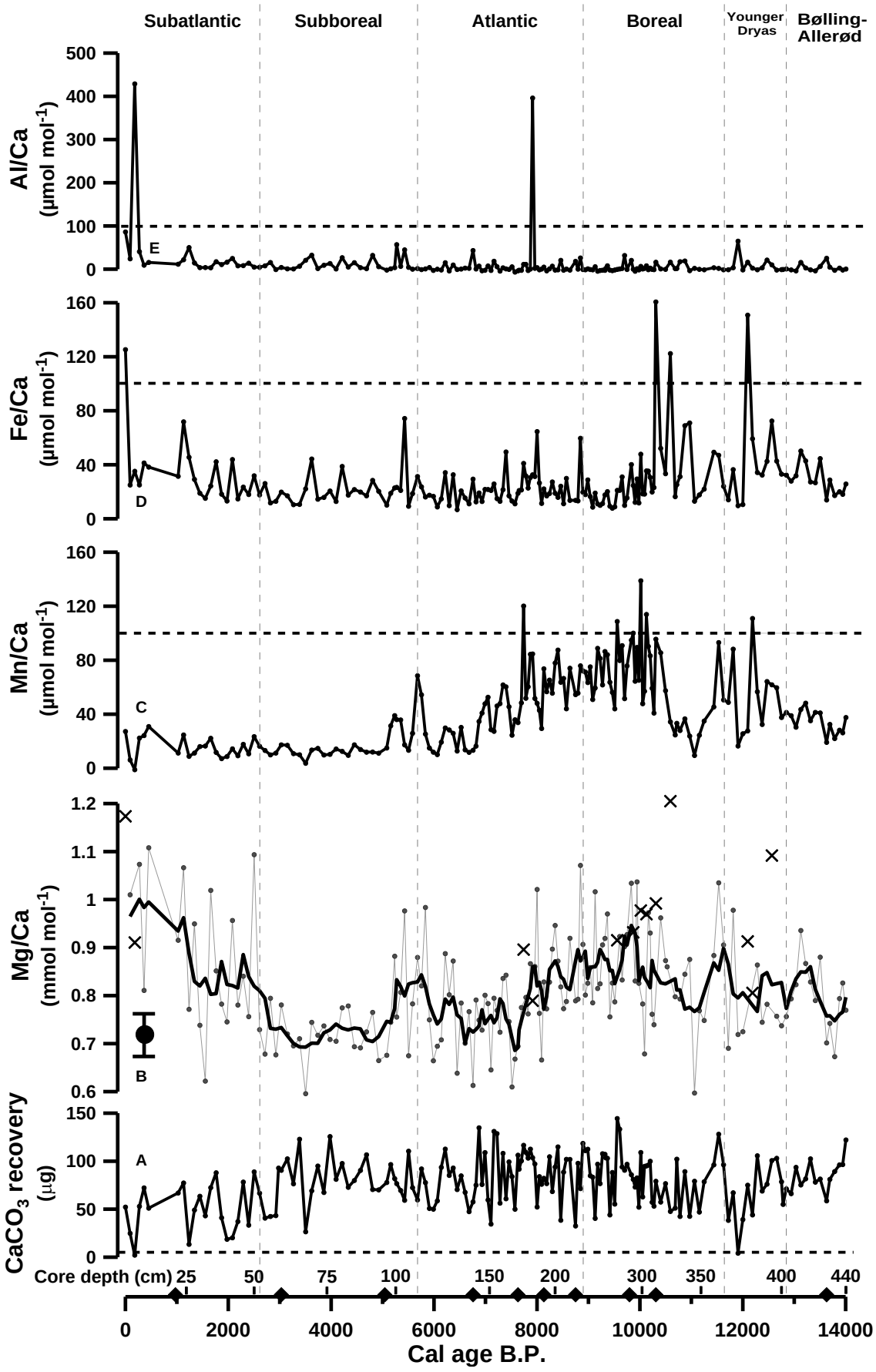
Subatlantic
Subboreal
Atlantic
Boreal
Younger Dryas
Bølling-Allerød
Al/Ca (µmol mol-1)
Fe/Ca (µmol mol-1)
Mn/Ca (µmol mol-1)
Mg/Ca (mmol mol-1)
CaCO3 recovery (µg)
A
B
C
D
E
Core depth (cm)
Cal age B.P.

Figure 6

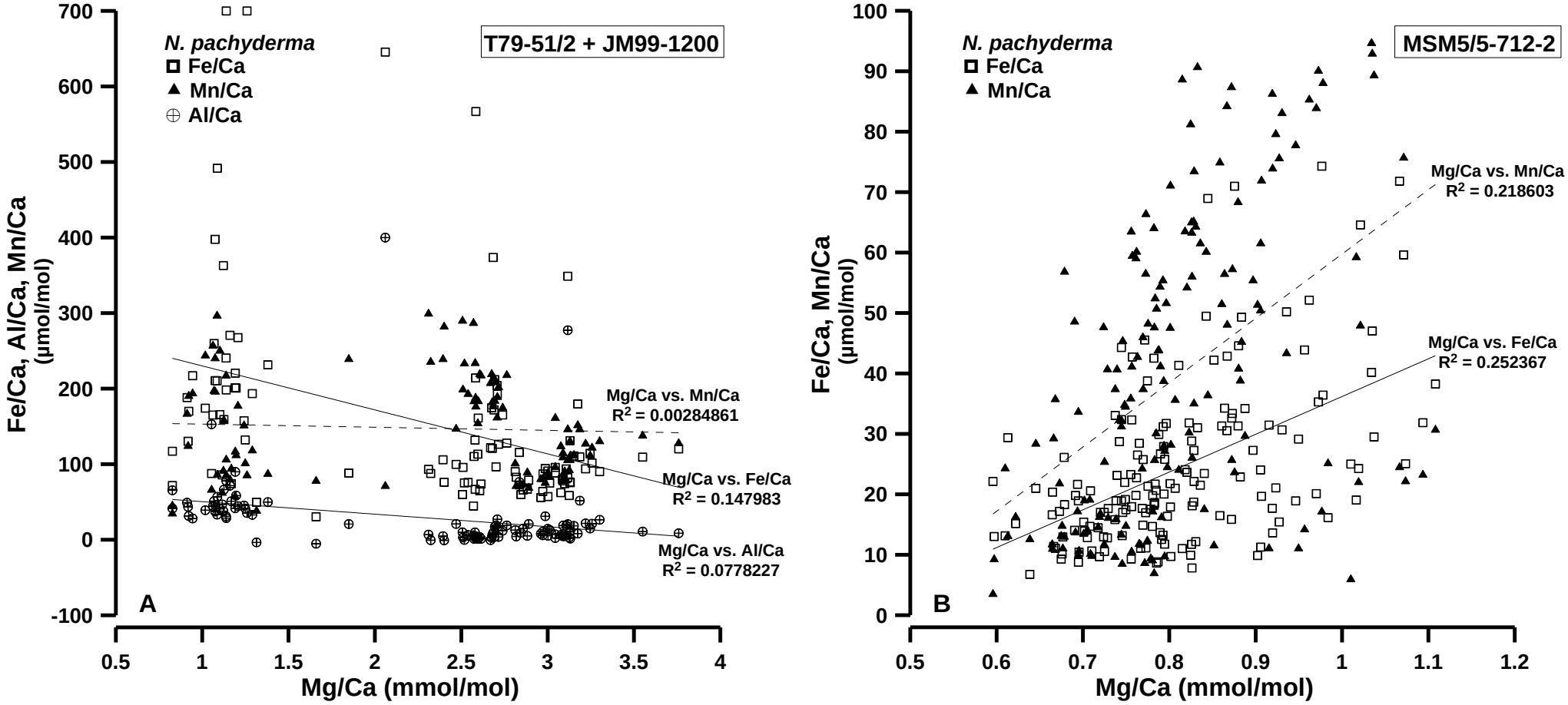
N. pachyderma
Fe/Ca
Mn/Ca
Al/Ca
T79-51/2 + JM99-1200
Mg/Ca vs. Mn/Ca
R2 = 0.00284861
Mg/Ca vs. Fe/Ca
R2 = 0.147983
Mg/Ca vs. Al/Ca
R2 = 0.0778227
Fe/Ca, Al/Ca, Mn/Ca (µmol/mol)
Mg/Ca (mmol/mol)
A
N. pachyderma
Fe/Ca
Mn/Ca
MSM5/5-712-2
Mg/Ca vs. Mn/Ca
R2 = 0.218603
Mg/Ca vs. Fe/Ca
R2 = 0.252367
Fe/Ca, Mn/Ca (µmol/mol)
Mg/Ca (mmol/mol)
B

Figure 7

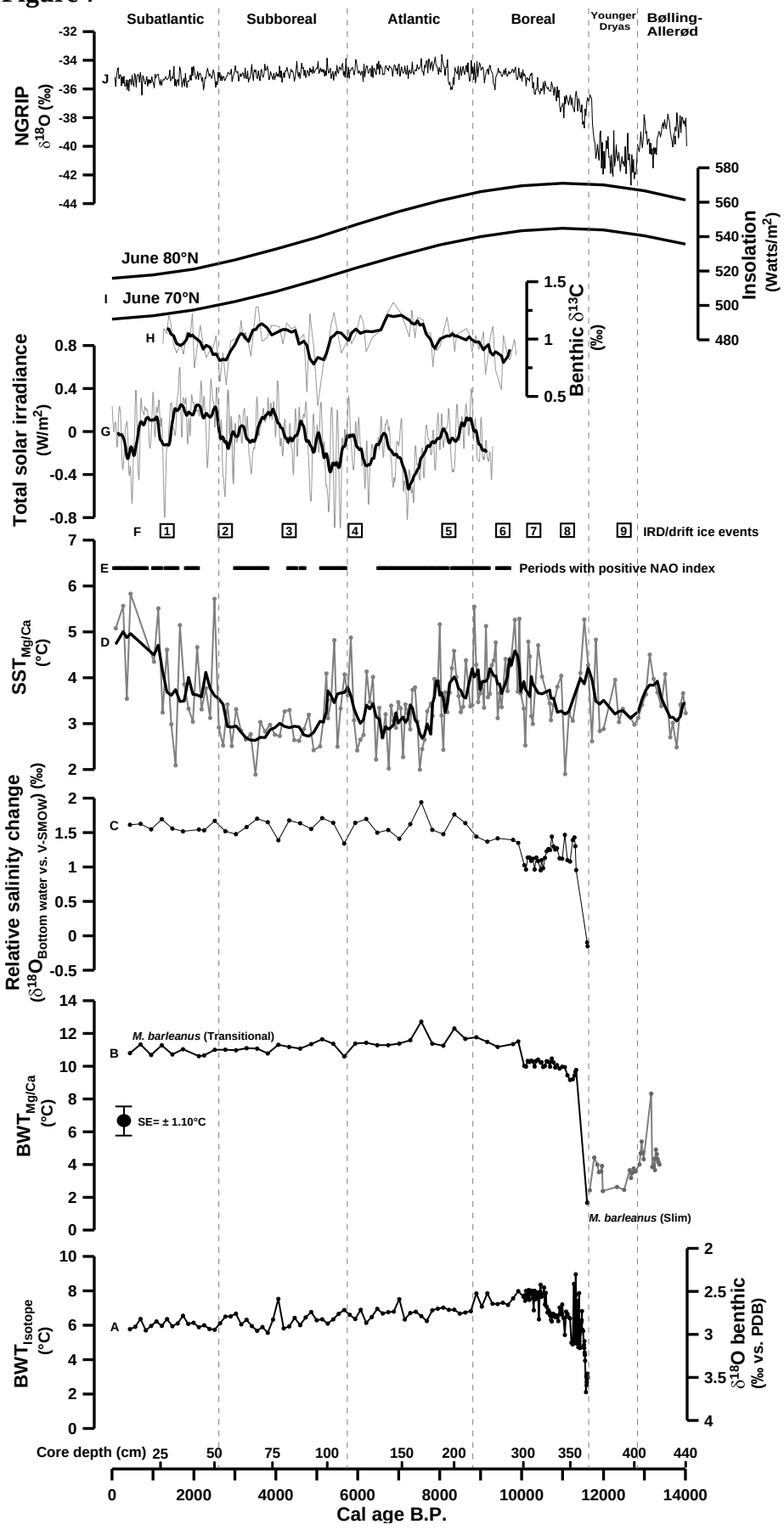
Subatlantic
Subboreal
Atlantic
Boreal
Younger Dryas
Bølling-Allerød
NGRIP δ18O (‰)
J
June 80°N
June 70°N
I
Insolation (Watts/m2)
Benthic δ13C (‰)
H
Total solar irradiance (W/m2)
G
F
1
2
3
4
5
6
7
8
9
IRD/drift ice events
E
Periods with positive NAO index
SSTMg/Ca (°C)
D
Relative salinity change (δ18OBottom water vs. V-SMOW) (‰)
C
M. barleanus (Transitional)
B
SE= ± 1.10°C
BWTMg/Ca (°C)
M. barleanus (Slim)
BWTIsotope (°C)
A
δ18O benthic (‰ vs. PDB)
Core depth (cm)
Cal age B.P.

Fig 8A. SiZer analysis of benthic $\delta^{18}O$ from the Andfjorden record (T79-51/2).

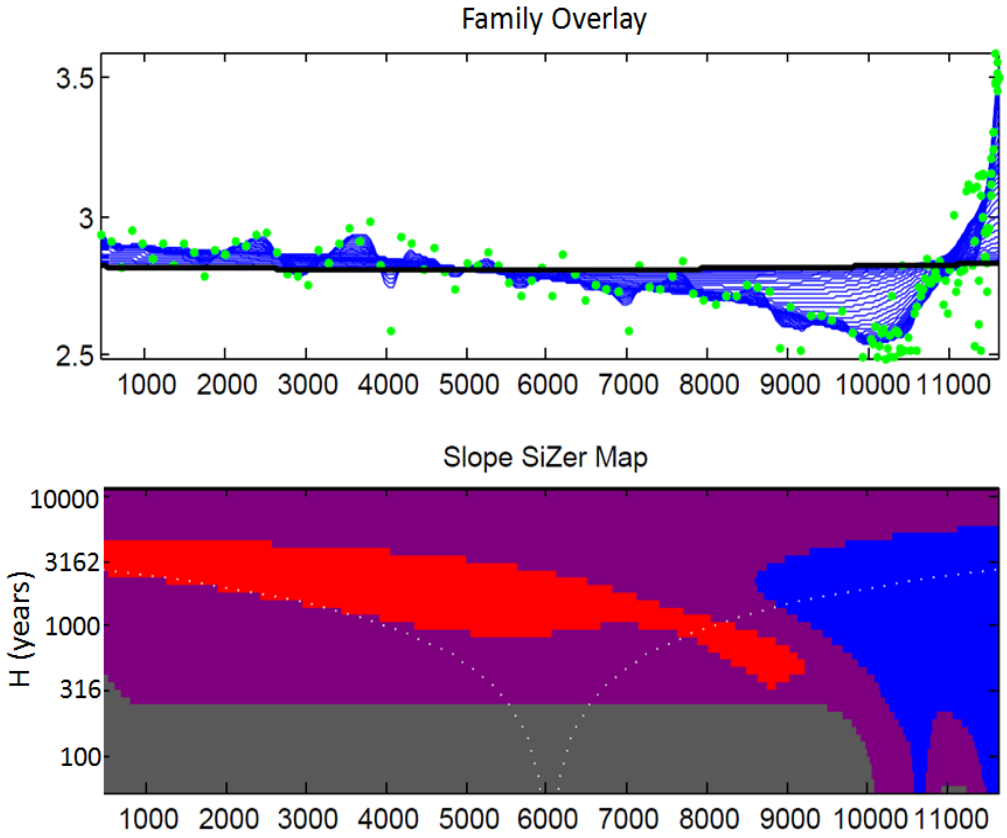

Fig 8B. TwoSiZer analysis based on $\delta^{18}O$ - Mg/Ca ratios from the Andfjorden record (T79-51/2).

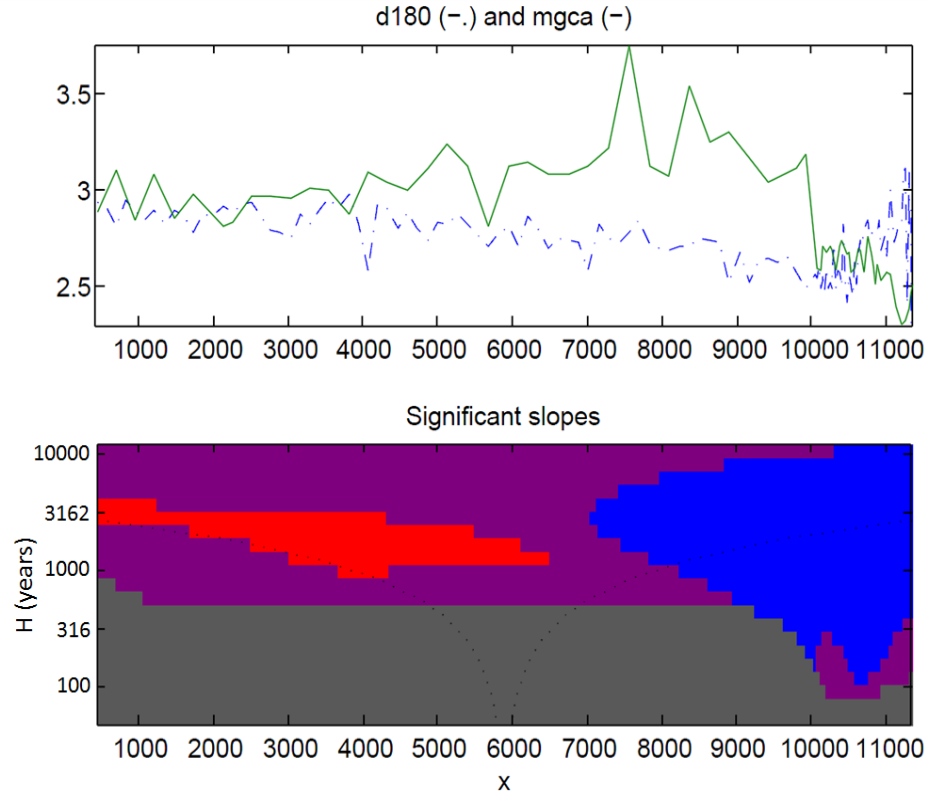

Fig 8C. SiZer analysis of the $BWT_{Mg/Ca}$ from the Andfjorden record (T79/JM99).

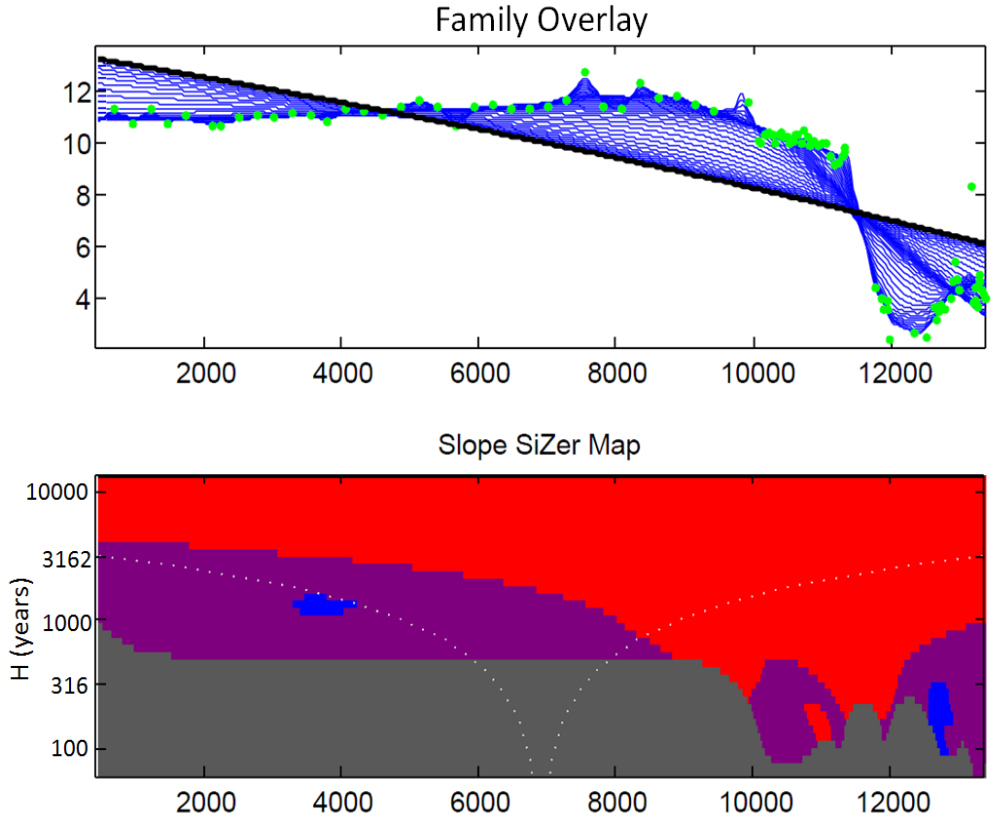

Fig 8D. SiZer analysis of $SST_{Mg/Ca}$ from the West Spitsbergen record.

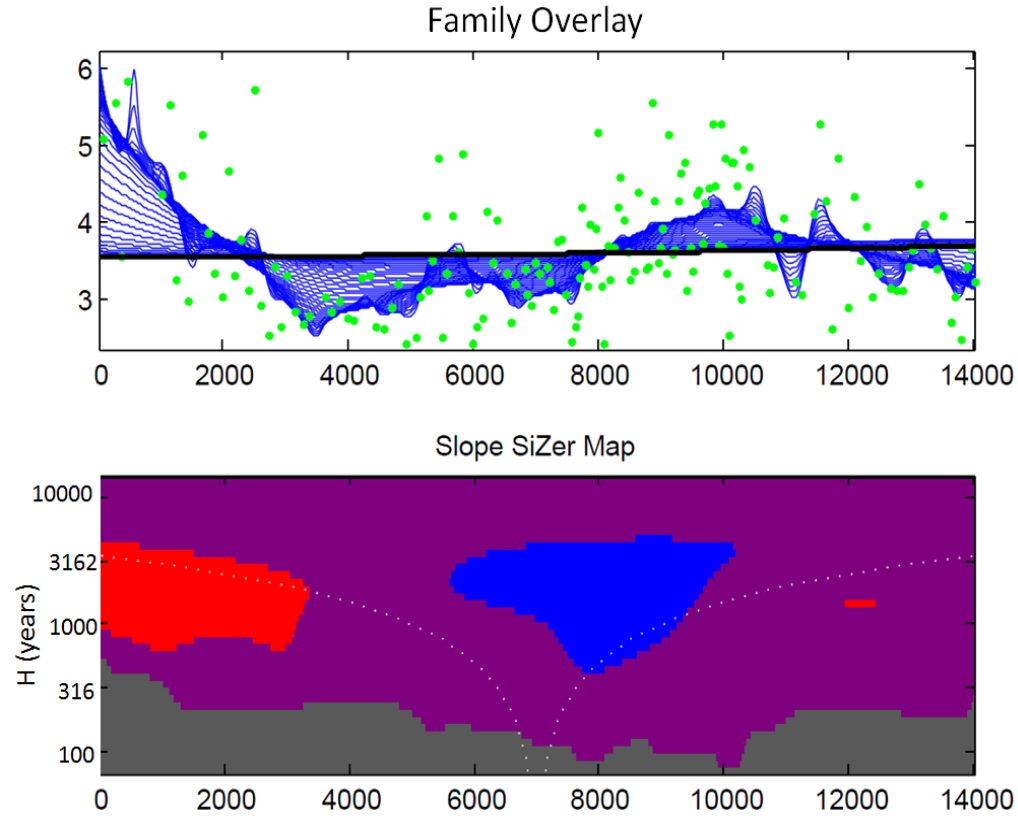

Fig 8E. TwoSiZer of $BWT_{Mg/Ca}$, (Andfjorden) – $SST_{Mg/Ca}$ (West Spitsbergen slope).